Improvement of the 1-D CFD Method for Thermal Management of a Battery Electric Vehicle

Master Thesis Report

Sashwat Chhetri (sasch884)

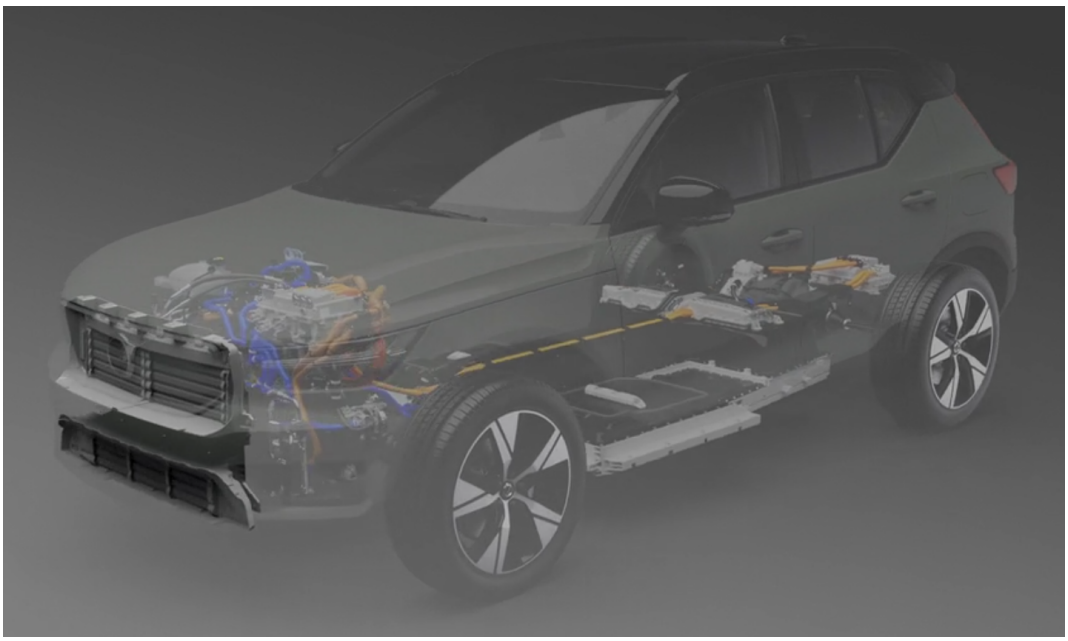

LINKÖPINGS UNIVERSITET

Linköpings universitet
Institutionen för ekonomisk och industriell utveckling
Examensarbete 2022|LIU-IEI-TEK-A–22/04268–SE

Linköpings universitet
Institutionen för ekonomisk och industriell utveckling
Ämnesområdet Mekanisk värmeteori och strömningslära
Examensarbete 2022|LIU-IEI-TEK-A–22/04268–SE

Improvement of the 1-D CFD Method for Thermal Management of a Battery Electric Vehicle

Master Thesis Report

Sashwat Chhetri (sasch884)

Academic supervisor: Jorg Schminder
Industrial supervisor: Karthik Narendra Babu
Examiner: Roland Gardgahen
Host Company: Volvo Car Corporation, Torslanda

LINKÖPINGS UNIVERSITET

Linköping universitet
SE-581 83 Linköping, Sverige
013-28 10 00, www.liu.se

Abstract

Electrification of vehicles is necessary to combat greenhouse gas emissions, which causes global warming and climate change. There has been a demand in the use of Battery Electric Vehicles due to this increased awareness of sustainability. However, they have been beset with issues such as range and conservation of energy. A part of the solution could be an energy-efficient thermal management system.
A 1-Dimensional (1-D) complete vehicle thermal model in GT-SUITE is used to predict the energy efficiency of the vehicle at the conceptual stage. The model helps predict results quickly and is used for complete system-level simulations. This thesis focuses on optimizing the method for predicting the realistic and accurate energy consumption of the thermal management system in the vehicle at the 1-D level. The Compact Modular Architecture (CMA) platform, which is the vehicle platform used in current production cars by Volvo Cars will be used for the study and all studies are performed using a standardized drive cycle. Initial sensitivity studies with a fully open grille are performed to understand the operating points of the various components of interest to investigate. The mass flow rate, ambient temperature, battery temperature, and cooling fan speed are varied.
The Active Grille Shutters (AGS) which provides aerodynamic benefit at high speed is implemented in the existing thermal model which could previously accommodate only the fully open grille. This allows the grille shutters to vary at different angles based on cooling demand. The previous existing thermal model method also needed to be optimized to accommodate the AGS. The cooling fan control logic needed to be improved for better accuracy and energy consumption prediction. Furthermore, the grille shutters and cooling fan speed is needed to regulate the amount of air flow through the heat exchangers for the model to behave as close to a real production vehicle. A code was developed which generated fan speed and grille shutter angles based on mass flow rate values to input in the model.
Further investigations were made with the optimized thermal model with AGS to study the influence of additional mass flow rate on the mass power consumption of the thermal management system components of interest. It was observed in the initial sensitivity studies that the additional mass flow rate saw significant power savings. However, with the implementation of AGS and additional mass airflow into the system, the power due to the variation of shutters is taken into account. The results indicate that the total power consumption gradually decreases with the increasing mass flow rate. But, this is up to a certain extent where the energy consumption due to the shutter opening takes over the overall power consumption of the vehicle and overcomes the savings seen by other components in the system causing the total power to increase.

Acknowledgements

This Master Thesis was conducted at the Thermal Efficiency Group, Volvo Cars Corporation (VCC). I would like to thank my manager Rosalie Olsson for providing me with an opportunity to work within this group. I am grateful to be provided the best facilities at the company for the thesis work to be carried out. I would express my sincere gratitude to my supervisor at VCC, Karthik Narendra Babu for all the guidance and support with the thesis work. I appreciate always receiving timely help with some of the challenges faced and getting up to speed with the tool. I would also like to thank Emil Willeson for the crucial inputs for the project work. I offer my gratitude to my group members for welcoming me and quickly making me feel part of the company. It has been an enriching experience learning from the best in the industry, which I would always cherish in the future.

I am grateful to my academic supervisor at LiU, Jorg Schminder for the feedback and help with the academic writing. I would express my gratitude to my examiner Roland Gardhagen for the approval of the thesis work and guidance throughout my master's degree.

Lastly, I would like to thank my family for their unconditional support throughout my studies. Additionally, I would like to thank my friends for their help in helping me settle in Sweden and for providing me with great company away from home.

Gothenburg, February 2022

Sashwat Chhetri

Nomenclature

Abbreviations and Acronyms

Abbreviation	Meaning
BEV	Battery Electric Vehicle
CO_2	Carbon Dioxide
AC	Air Conditioning
VCC	Volvo Cars Corporation
CMA	Compact Modular Architecture
LiU	Linköping University
CAE	Computer Aided Engineering
IC	Internal Combustion
CFD	Computational fluid dynamics
1-D	One-Dimensional
3-D	Three-Dimensional
AGS	Active Grille Shutters
ED	Electric Drive
EWP	Electric Water Pump
GT	Gamma Technologies
CVTM	Complete Vehicle Thermal Model
HVAC	Heating Ventilating Air Conditioning
RPM	Rotations Per Minute
PID	Proportional Integral Derivative
PWM	Pulse Width Modulation
WLTC	Worldwide Light Vehicle Test Cycle
KWH	Kilo Watt Hours
VCU	Vehicle Control Unit
NVH	Noise Vehicle Harshness
EPS	Electric Propulsion System
HV	High Voltage

Latin Symbols

Symbol	Description	Units
A	area	$[m^2]$
p	Pressure	$[Pa]$
t	Time	$[s]$
k	Thermal Conductivity	$[W/mK]$
L	Thickness	$[m]$
T	Temperature	$[°C]$
h	Heat Transfer Coefficient	$[-]$
F	Force	$[N]$
V	Velocity	$[m/s]$

Symbol	Description	Units
C_D	Coefficient of Drag	$[-]$
P	Power	$[W]$
$\dot{m}$	Mass Flow Rate	$[kg/s]$

Greek Symbols

Symbol	Description	Units
α	Angle	$[degree]$
σ	Stefan Boltzmann Constant	$[-]$
ε	Emissivity	$[-]$
ρ	Density	$[kg/m^3]$

Contents

1 Introduction

The number of greenhouse gases added to the atmosphere per year due to human activities amounts to 51 billion tons [1]. The higher concentrations of greenhouse gases and carbon dioxide in particular, are causing extra heat to be trapped and global temperatures to rise on our planet. These emissions need to be brought down to zero, as reducing emissions will just delay the disastrous impacts of climate change. The transportation sector is one of the prime emitters of these gases. It is projected by the mid-century mark, greenhouse gas emissions from transportation must be at least 60% lower than in 1990, to be firmly on the path to zero [2]. In 2018, light-duty vehicles account for 15% of total CO2 emissions in the European Union [3]. These light-duty vehicles (passenger cars and vans) contribute the most to greenhouse gas emissions in the transportation sector, followed by heavy-duty vehicles (trucks and buses), maritime navigation, and aviation.

Battery Electric Vehicles (BEVs) are growing rapidly in demand with increased awareness of the effects of global warming. These vehicles have a battery-powered electric motor instead of an internal combustion engine. Although their environmental impact is higher during production than internal combustion engine vehicles, their overall life cycle seems to be cleaner. BEVs promote green economy thanks to the simple fact that they produce zero tailpipe emissions, thus making their impact cleaner, better and more advantageous for the environment than combustion engine vehicles. Hence they are referred to as zero-emission vehicles. These vehicles also have a highly efficient conversion ratio (battery energy to traction) offering tremendous power with some of the fastest cars in the world electric powered. With the induction of cleaner sources of energy, BEVs could potentially be a game changer for the climate crisis. Increasing environmental regulations have also led to most automotive manufacturers pushing towards electrification. The trend of the automotive market moving to greener vehicles is indicated by the sales of both BEVs and Plug-in Hybrid Vehicles have increased 100 times in 2015 more than 2010 [4]. Volvo Car Corporation (VCC) aims to be part of this electric revolution moving to fully electric cars by 2030, phasing out all combustion and hybrid vehicles.

However, BEV's have been plagued with issues such as range and conservation of energy. They are particularly susceptible to severe temperatures, resulting in reduced driving range, particularly in colder areas. They are key hurdles to achieving wide consumer acceptance along with vehicle cost. Over half of the energy in a car is lost to various cooling systems, which include the engine cooling system, air conditioning system (AC), frictional component cooling, and exhaust gas cooling [5]. One part of the solution can be an energy-efficient system like for the vehicle thermal management system to cut the energy losses. With the right thermal management design setup, electric vehicles could benefit with better range and comfort. Therefore, superior driving performance for the customers. This could make BEV's more affordable as well, encouraging more customers to make the shift from traditional Internal Combustion (IC) engine vehicles ensuring a sustainable future for the planet.

1.1 Background

With the ever-increasing demand for the use of electric cars in the future, a need arises for an energy-efficient thermal management system. The thermal management system is responsible to keep all the components within their temperature limits to ensure functionality and safety of the vehicle, while also generating pleasant temperatures for passengers in the vehicle interior. These components work more efficiently consuming less energy as well, if operated within the respective limits. Hence this system is decisive in determining the performance and the conservation of energy to increase the range of the vehicle, which is a major challenge right now for most BEV's.

By improving the thermal management system simulation method, an efficient system could be designed which can consume less energy and increase the performance of the vehicle. This is possible with the help of Computer Aided Engineering (CAE) tools. With the help of 1-Dimensional (1-D) simulation tools each component can be studied and its effect on the thermal management system can be quantified. A 1D-CFD (Computational Fluid Dynamics) simulation also known as system-level CFD focuses on the outputs of the overall system, for e.g the entire thermal management system of the vehicle rather than the specifics of the flow inside a single component of the system. These tools help in the modeling of the full thermal model, allowing problems to be examined and solved from the perspective of the entire system. Because system-level simulations require only a few seconds or to a few hours to perform, it is feasible to test hundreds or even thousands of various configurations, operational conditions, and maneuvers throughout the pre-design and design phases. A 1D-CFD method using a solver such as GT-SUITE offers the ability to do transient simulations at very short interval of time for drive cycles as opposed to 3D-CFD, where it could not be possible or could take a long duration of simulation time owing to computing constraints.

The results provide engineers with a good understanding of the entire system's performance and its sensitivity to different conditions at the initial conceptual stage [6]. The 1D-CFD method however, is an evolving method with certain simplifications to model the actual components which affect the accuracy of the results. Various components are not modeled in the system for simplicity. To make better energy predictions at the conceptual level for these vehicles, an accurate method must be implemented ensuring the correct approach and control replication of the real components at the 1-D system level. Improvement of the 1D-CFD thermal model and simulation method would help in yielding more accurate results at the system level. As a result of defining the correct method, accurate energy predictions can be made quickly, therefore speeding up the design and analysis process in vehicle development.

Active Grille Shutters (AGS) are implemented in most production vehicles to influence the airflow in the thermal management system of the vehicle. The Active Grille Shutters allow airflow through the grille when demand on cooling system or air conditioning system is high [7].Under conditions of light load and moderate ambient temperatures and humidity, the grille does not have to be fully open therefore decreasing the drag on the vehicle. The physical behavior of the shutters is implemented in the thermal models for the study. These shutters regulate the cooling airflow in the vehicle, with this cooling airflow affects the aerodynamic drag of the vehicle. It is important to model this system in the thermal model to make more accurate energy estimations of the BEV.

Therefore this system is implemented in the current thermal model. Aerodynamic resistance is one of the major factors in reducing energy consumption of a vehicle [8]. This is investigated further in the study.

1.2 Literature Review

1-D Computational Fluid Dynamics is a flexible approach to perform simulations and is being used to study models at a system level. A study done by Arturo et.al [9] performed a 1-D study to predict the compressor, battery load consumption and compared them to test data for a specific drive cycle. They observed a nominal difference of 6.25 % justifying simulation data to be near as accurate. Okamoto et.al [10] in their work optimized a way to control the heat flow from the engine and heat pump using a 1-D vehicle thermal model for a hybrid electric vehicle and achieved a 10 % improvement in energy efficiency to a conventional vehicle. Dinakar et.al [11] successfully modeled the cooling systems of a battery using GT-suite 1-D models at a system level for various drive cycles for efficient power consumption of batteries and states that a complete vehicle thermal model perspective could be useful. The studies performed by Arturo et.al [9], Okamoto et.al [10], Dinakar et.al [11] show that 1-D simulations give reasonably accurate results to perform thermal model simulations.

In the past decade, a lot of studies have been done on active grille shutters. It has been a hot topic on automobiles for its impact in the field of engine cooling, cabin cooling, energy management and fuel economy. El-Sharkawy et.al [7] evaluated the impact of the active grille shutter on powertrain cooling and underhood components. They analyzed the power consumption from the thermal management components and were successful in implementing a strategy for when the shutters should be closed/open based on the component demand. Natarajan et.al [12] investigated the influence of active grille-shutter on the air conditioning system where at different driving scenarios the power consumption was analyzed at various ambient temperatures giving based on the conditions about 7-10 % decrease in power consumption. Bouilly [13] performed a study for evaluation of fuel economy potential of an Active Grille Shutter for vehicle heat management achieved about 1.7 % to 2.4 % percent fuel economy based on drive cycles.

J.Nordin [14] performed a CFD study related to thermal management of underhood flow for electric vehicles to determine the idea and design configuration that provides the least amount of cooling drag for a given mass flow rate. Martini et.al [8] analyzed the effect for different front-end designs of a truck by evaluating the drag and the radiator top tank temperature where an open grill influenced a better cooling but caused an increase in drag of the vehicle. Yang [15] also evaluated the Impact of front-end Air Flow Conditions on AC Performance and fuel consumption of vehicles with AGS which resulted in a method that saw improvement in fuel consumption of up to 0.7 % then a fully open grille case.

Various studies like the above have been done to show the influence of the active grille shutter on the thermal management system and its benefits. The author [12] recommends integrating the active grille shutters with the entire system model and fan models, which will be done for this study. Yang [15] recommended AGS and cooling fan increase will lead to energy savings. Hence the credibility of performing 1-D CFD simulations involving the use of AGS and cooling fan for optimizing the existing thermal model on the thermal management system have been quantified for this project.

1.3 Aim

The main objective of this thesis is to improve the currently used 1-D Computational Fluid Dynamics (CFD) simulation method at VCC to perform more accurate estimations of the power consumers in the thermal management system for a Battery Electric Vehicle (BEV). This study involves the implementation of active grille shutters and an enhanced cooling fan algorithm into the complete vehicle thermal model, along with an improved simulation method. This improvement helps make better energy predictions, as the thermal model works as similar to the thermal management system would work in the real production vehicle. Furthermore, simulations are performed under certain load cases in conventional driving conditions to investigate the effect of these load cases on the overall energy efficiency of the vehicle. This study would help develop better cooling strategies in the future.

1.4 Resources and Limitations

- The thesis work is limited to 20 weeks as part of the project work (TQFT30) for the Master in Aeronautical Engineering course at Linkoping University.
- The simulations are performed using the 1-D software GT-Suite and will be simulated on a cluster provided by Volvo Cars for faster processing time.
- A Complete vehicle thermal model will be used to perform the simulations wherein the model is provided by the company.
- Some of the components are not modeled and rely on maps with data for working.
- It is out of the scope of the thesis to make any design changes to the model components.
- Simulations could be performed for various types of drive cycles but is limited for a single type.
- The model has been studied for only a cool-down case scenario, where the vehicle cabin temperature is at a high temperature and needs to be brought down to a lower temperature.
- The investigations lack any data for validation purposes due to being in its conceptual phase.

2 Theory

2.1 Computational Fluid Dynamics

Computational Fluid Dynamics (CFD) is the computer-based analysis of systems involving fluid movement, heat transport, and related phenomena such as chemical reactions. This technique is quite powerful and is employed in both industrial and non-industrial applications [16].

CFD simulations allow simulating real and ideal conditions, that would generally be not easily tested in real life. It is relatively inexpensive, and costs are likely to decrease as computers become more powerful [17]. It provides comprehensive information from regions of specific interest of the study. The simulations can save a lot of time in the early design and conceptual phase, as compared to experiments.

All of CFD, in one form or another is based on the fundamental governing equations of fluid dynamics-the continuity, momentum, and energy equations. The equations here are solved in one dimension, which means that all quantities are averaged across the flow direction. The conservation equations that are used are shown in eq.(1)(2)(3)

$$\text{Continuity:} \quad \frac{dm}{dt} = \sum_{\text{boundaries}} \dot{m} \tag{1}$$

$$\text{Energy:} \quad \frac{d(me)}{dt} = -\rho \frac{dV}{dt} + \sum_{\text{boundaries}} (\dot{m}H) - hA_s \left(T_{\text{fluid}} - T_{\text{wall}}\right) \tag{2}$$

$$\text{Momentum:} \quad \frac{d\dot{m}}{dt} = \frac{dpA + \sum_{\text{boundaries}} (\dot{m}u) - 4C_f \frac{\rho u|u|}{2} \frac{dxA}{D} - K_p\left(\frac{1}{2}pu|u|\right)A}{dx} \tag{3}$$

There are two choices of time integration methods, which affect the solution variables and limits on time steps, explicit and implicit integrator. Explicit methods are used when the primary solution variables are mass flow, density, and internal energy. Implicit methods are used when the primary solutions are mass flow, pressure and total enthalpy.[18] The explicit solver is generally used when the wave dynamics are important for example in engine, acoustics, and fuel injection and the other is the implicit solver which is used when high-frequency wave dynamics are not important and Mach number is less than 0.3, for instance, cooling, air conditioning, and map-based lubrication.

Discretization takes place of the domain, where it is divided into one or more volumes. It is the process of dividing big elements into smaller sections in order to get an appropriate solution.[19] This system is subjected to the governing equations, and the solver computes scalar values such as temperature, pressure, and enthalpy, as well as vector quantities such as velocity and mass flux [18].

2.2 Heat Transfer

All matter contains thermal energy. The more motion the atoms or molecules have, the more heat or thermal energy they will have. Heat Transfer describes the flow of heat due to temperature changes. There must be a temperature difference between the two bodies for heat transfer to occur. Without this difference, no heat transfer can take place. The study of transport phenomena involves the exchange of momentum, energy, and mass in the three forms of heat transfer. The modes of heat transfer are conduction, convection, and radiation.

2.2.1 Conduction

Conduction is the method of transfer of heat within a body or from one body to the other due to the transfer of heat by molecules colliding against each other. The bodies through which the heat transfer must be in contact with each other. Fourier formulated a theory for conduction which stated the heat flux, q (W/m^2) which is the heat flow per unit area is proportional to the magnitude of the temperature gradient and opposite to it in sign. Based on the denotation of constant of proportionality k, then

$$q = -k\frac{dT}{dX}$$

The constant k, is called the thermal conductivity having the dimensions W/mK.

For one-dimensional heat conduction problems, it is clear that the direction of heat flow is from hot to cold. Hence Fourier's law is written in the simple scalar form:

$$q = k\frac{\Delta T}{L}$$

where L is the thickness in the direction of heat flow and q and ΔT are both written as positive quantities [20].

2.2.2 Radiation

Radiation is another form of heat transfer. It does not require any medium and can be used for the transfer of heat in a vacuum as well. This method uses electromagnetic waves that transfer heat from one place to the other.

A Black Body refers to a body which absorbs all electromagnetic radiation and in order for it to stay in thermal equilibrium must emit radiation at the same rate.[21] The Stefan Boltzmann law indicates that the thermal energy radiated by a blackbody radiator is proportional to the fourth power of the absolute temperature and is given by:

$$E = \sigma T^4$$

where E is the radiant heat energy emitted from a unit area in one second, T is the absolute temperature σ is the Stefan Boltzmann constant [20].

To calculate the total power of the body's thermal radiation (which the average power emitted per unit are of radiating body), its surface area is considered A in (m^2)

$$P = \sigma \varepsilon A T^4$$

where the constant, ε is less than 1 for gray bodies which are considered imperfect. But for simplification, the constant ε is set to 1 by assuming the object is a perfect black body.[22]

2.2.3 Convection

Convection is the mode of heat transfer that occurs in liquids and gases. In this method, heat transfer takes place with the actual motion of matter from one place within the body to the other. When fluid forms a thin slowed-down region called the boundary layer adjacent to the body, heat is conducted into this layer which vanishes and mixes into the stream. This heat is often carried away by a moving fluid due to convection.
The steady-state form of Newton's law of cooling defines convection for all convective flows by the formula:

$$Q = hA(T_b - T_\infty)$$

where h is the heat transfer coefficient, A is the heat transfer surface area, T_∞ is the temperature of the incoming fluid, T_b is the temperature of the body [20].
Convection can be classified as forced or free. Forced convection is caused when the fluid is moved with the help of an external means such as a fun or a pump. Natural or free convection is caused due to the instance of buoyancy effects.

2.3 Aerodynamics

Aerodynamics is a branch of fluid dynamics that deals with the motion of air, with the forces acting upon an object in motion through the air, or with an object which is stationary in a current of air [23]. Aerodynamics plays a big part in vehicle engineering as if a vehicle can move past the air smoothly there is a prospect of lowering energy consumption. Under aerodynamics, the dominating forces acting on the vehicle are lift and drag. Lift is the force generated perpendicular to the motion of travel for the body when it interacts with the fluid. Drag is the opposing force acting as a consequence of the motion of a body moving through a fluid. Lift coefficients and drag coefficients are dimensional quantities used to signify lift and drag. They are constantly evaluated to calculate the aerodynamic performance of vehicles.

The two primary types of drag are the pressure drag or the form drag and the skin friction drag. The form drag is caused as a result of the shape and size of the vehicle. Skin-friction drag is generated by the traction due to shear stresses acting on the body surface. This traction is due to viscosity and acts tangentially at all points on the surface of the body [24]. Aerodynamics drag force is the drag due to the vehicle's motion through the fluid.

It is the resistance force applied by the flowfield of air traveling in the opposite direction on a moving object. The aerodynamic drag F_{aero} is represented by the equation:

$$F_{aero} = \frac{1}{2}\rho_{air} C_D A V^2$$

where C_D is the coefficient of drag, ρ_{air} is the density of ambient air, V is the velocity of the body and A the frontal area. The power needed to overcome this drag force is P_{aero}. This power consumption due to the force is calculated by the equation:

$$P_{aero} = F_{aero} * V$$

2.4 Thermal Management System Components

2.4.1 Compressor

The compressor is a key component of the refrigerant circuit and the heart of the air conditioning system. The role of this component is to regulate the flow of the refrigerant in the circuit. In action, the compressor takes the low-pressure refrigerant from the evaporator and compresses it according to vehicle speed and air temperature. The inlet side is known as the low (pressure) side and the outlet side is known as the high (pressure) side. The compressor compresses the refrigerant, raises its temperature and pressure to force the refrigerant into the heat exchangers where the heat transfer takes place. The compressor is shown below in Fig. 1.

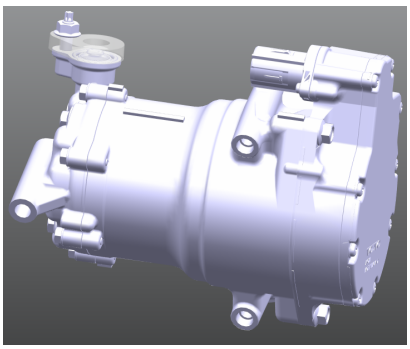

Figure 1: Compressor

2.4.2 Condenser

The condenser acts as a heat exchanger that is mounted in front of the vehicle, behind the grill. It uses air that is brought in from the fan or vehicle movement to transfer heat. It contains a multitude of cooling fins, which the coolant passes through. The highly pressurized refrigerant coming from the compressor flows into the condenser, transfers heat, and warms it. This causes the condenser to be hotter than the forced air coming through the condenser. The condenser hands its heat off to the forced air and turns the refrigerant back into cool liquid in the expansion valve, where it heads back to the evaporator.

2.4.3 Radiator

The radiator is another heat exchanger used in the cooling package in the car. Radiators are used in the vehicle to accommodate the cooling needs of both the battery and the electric drive components. Automotive radiators consist of two end tanks (inlet and outlet), which hold the cooling fluid, and a core. The core of a radiator is comprised of tubes and fins.
The tubes run lengthwise from tank to tank and the fins are located in the spaces between the tubes. The radiator consists of cooling fins where the heat transfer between the coolant and air takes place. The hot coolant comes in contact with the air and cools due to convection therefore, reducing the temperature of the coolant. The cooling package is shown in Fig. 2.

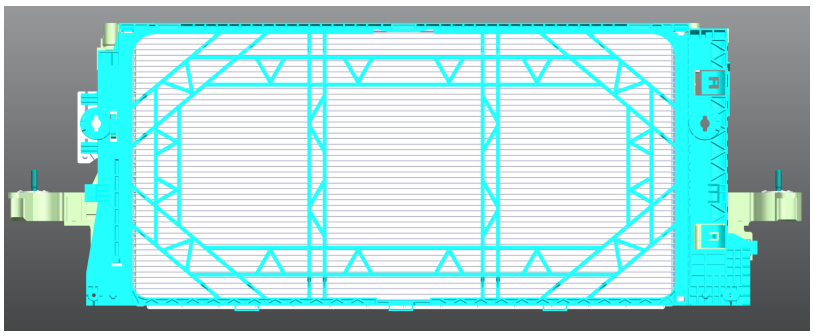

Figure 2: Cooling Pack that consists of Radiator and Condenser

2.4.4 Evaporator

The evaporator is another component just like the condenser, acts as a heat exchanger. It is the only component of the AC system that is located in the passenger cabin, behind the dashboard. When the refrigerant enters the evaporator it is in a liquid state. A fan blows warm air over the evaporator. The warm air causes the liquid refrigerant to boil. This means that it absorbs the heat from the warm air. Once it has absorbed the heat from the warm air, the warm air isn't warm anymore and is cold. This air is passed to the cabin of the car and provides air conditioning.

2.4.5 Cooling Fan

The cooling fan is the fan placed behind the radiator. It allows a great flow of air to pass through the radiator ensuring the refrigerant is kept at an optimal temperature under all vehicle conditions. The fan is controlled via pressure or temperature switches or a control unit. The electric radiator fan or fans are usually mounted on fan shrouds. These shrouds have the task of guiding the air flowing through the heat exchangers to the fan in a targeted manner and as free from flow losses as possible. For this reason, the fan shroud is also mounted as close as possible to the radiator. The cooling fan is shown below in Fig. 3.

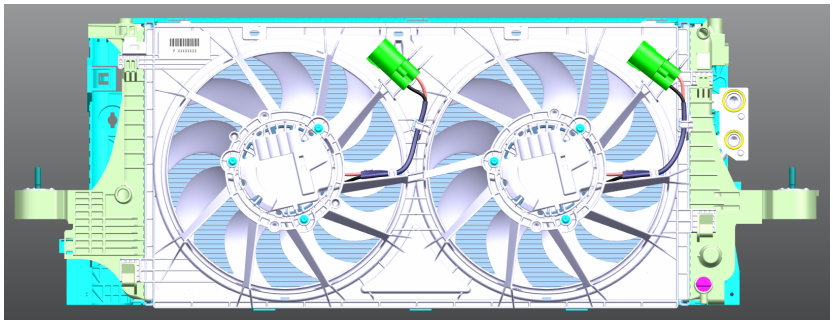

Figure 3: Cooling Fan

2.4.6 Chiller

The chiller is a special heat exchanger connected to both the coolant and refrigerant circuits, which allows the temperature of the coolant to be further reduced by the refrigerant in the air-conditioning system. This allows additional indirect cooling of the electric motor and the power electronics by the air-conditioning system if required. The use of a chiller comes in handy during conditions when the radiator is not able to cool down the battery on its own, i.e. during high load and ambient temperature conditions. The chiller is shown in Fig. 4.

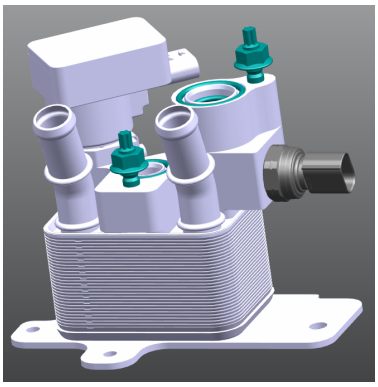

Figure 4: Chiller

2.4.7 High Voltage Coolant Heater

As the electric vehicle does not receive any hot exhaust heat from the engine, the heater is used to heat the coolant when the temperatures become too low for the battery and other components. The coolant is heated via an electrical auxiliary high-voltage heater that is integrated into the cooling circuit. The temperature distribution between battery packs and cells remains continuously homogeneous due to the low thermal mass that enables fast reaction times for heating up and cooling down.

2.4.8 Pumps

Pumps can be mechanical or electric. For electric vehicles, electric water pumps are used. Electric water coolant pumps and their integrated electronic control are variably activated according to the required cooling needs. It helps move the coolant from the radiator to all the necessary parts in the powertrain. By utilizing a controller, it can determine how much coolant circulates through the engine at given temperature ranges and maintain a target temperature. This prevents inadequate or excessive cooling. They can be used as main, minor, or circulation pumps. The primary pumps taken into account here are the Battery Electric Water Pump and the Electric Drive Electric Water Pump (ED EWP). The battery EWP is used to regulate flow of coolant into the chiller and battery components. The ED EWP does the same job for the electric drive i.e the electric motor. Based on the coolant temperature values the pump speed is regulated. The electric water pump is displayed below in Fig. 5.

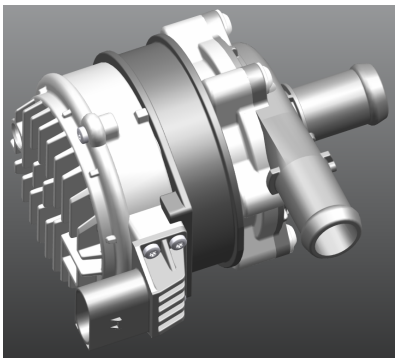

Figure 5: Electric Water Pump

2.5 Thermal Management System in BEV's

The Thermal management system of a Battery Electric Vehicle (BEV) regulates the heat flows inside the vehicle. The corresponding components of the system need to be operated in their respective optimal temperatures while generating pleasant temperatures for the passengers in the vehicle interior. The thermal management system for a BEV as seen in Fig. 6 consists of the electric drive unit, battery cooling and cabin cooling components. The system is more complex in an electric vehicle as compared to a combustion engine due to the battery being the primary source of energy. The battery of an electric vehicle needs to be cooled or heated all the time depending on the ambient conditions. Scenarios such as fast charging as well could overheat up the battery when the vehicle is stationary. Various pumps are also required to regulate flows in the circuits. No waste heat is also available to heat the interior from the combustion engine, so heat pumps are required to be added which require additional components in the vehicle. [25]

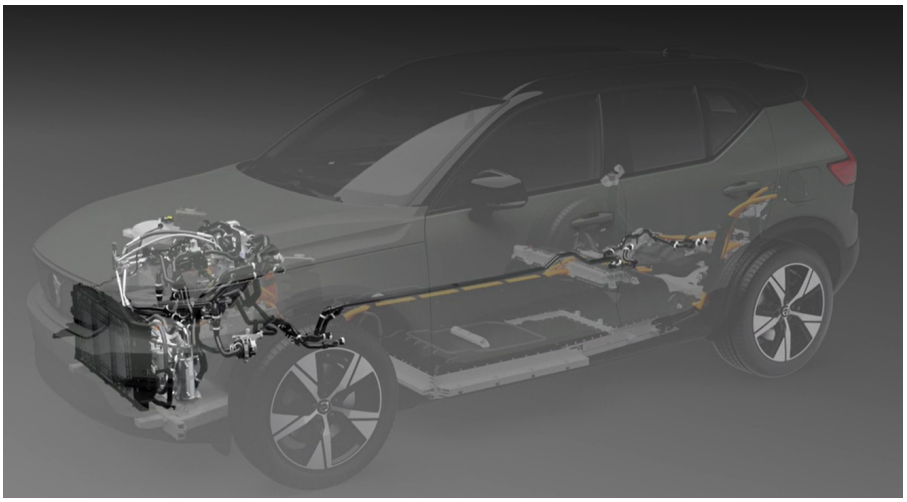

Figure 6: XC 40 Recharge Cooling System and Components

The refrigerant circuit is responsible for the cabin cooling. It is a liquid that contains a very low boiling point. A refrigerant is circulated in the refrigerant circuit which can be both liquid and gaseous. It is powered by an electronic compressor that compresses the refrigerant to the requisite pressure, enabling evaporation and condensation at the chosen temperature levels. The refrigerant gas is compressed to high pressure and high temperature in the compressor. This gas is passed through the condenser where heat rejection takes place on interaction with the heat exchanger turning it to the liquid state. Next, the liquid refrigerant moves to the drier which removes moisture. The refrigerant then travels to the expansion valve, where the pressure in the line is decreased and the refrigerant is converted back to a gaseous condition. The colder refrigerant is still in gas form as it then enters the evaporator. Heat is removed from the air and transferred into the refrigerant when air is forced through the evaporator core, resulting in cooler air being pumped into the passenger compartment. The refrigerant is again passed through the compressor and the repeat cycle continues.

The coolant circuit cools the battery and the electric drive units. The Electric Drive (ED) unit consists of the propulsion components such as Electric Front and Rear Axial Drives etc. The coolant is circulated by a pump in the cooling circuit and transports heat to the corresponding component that requires it inside the vehicle. When coolant absorbs heat, its temperature rises and needs to be cooled in a heat exchanger. For battery cooling the chiller and other components such as heaters, pumps will be used depending on whether it is a cool-down or heating up case. Batteries can be cooled either by liquid cooling or air cooling. For air cooling a passive air-cooling system is used , which uses outside air and the movement of the vehicle to cool down the battery without the need of an external power source. For liquid cooling, piped liquid cooling systems are used for battery thermal management which might use an external power source. Liquid cooling provides better cooling as they conduct more heat away from the batteries but the downside is it limits the air that can flow through the battery.

As shown in the Fig. 7 the refrigerant circuit (Climate circuit) and coolant circuit (ED and battery circuit) must work hand in hand depending on the heating and cooling requirements. For example, if sufficient flow is not happening across the condenser, then the performance of condensers comes down and optimum temperature around battery packs cannot be maintained. The interconnection changes between these two circuits depending on whether the vehicle needs to be cooled or heated.

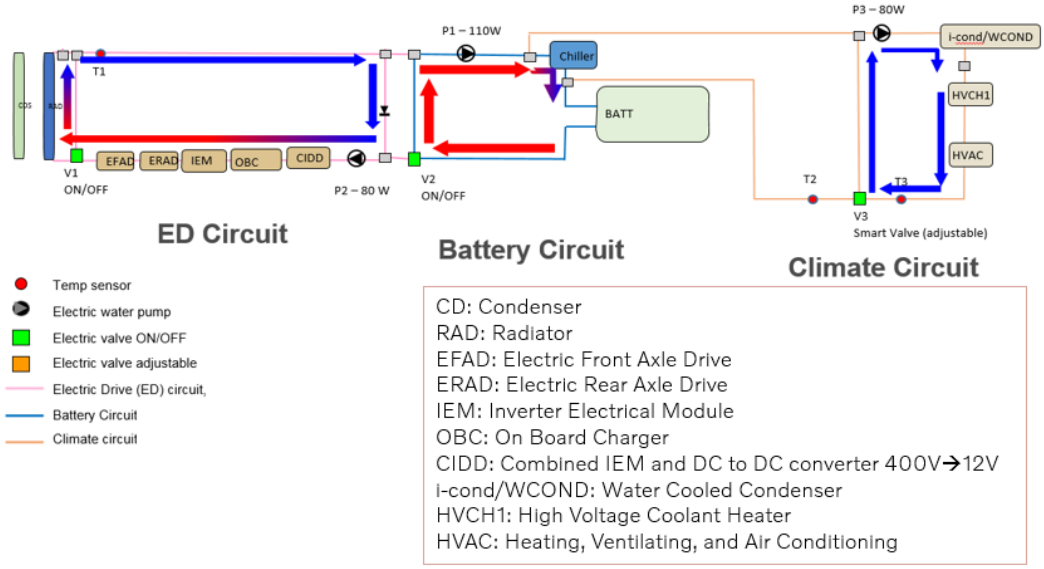

Figure 7: CMA Platform Vehicle Circuits

2.6 Active Grille Shutter System

The Active Grille Shutter (AGS) is located at the front bumper lower opening. This system controls the amount of airflow through the shutter into the vehicle underhood via a flap which is operated by an actuator that receives signals. While driving at certain speeds, the active grille shutter system closes the shutter to reduce airflow to the engine compartment to reduce the aerodynamic drag and as a result, improves the vehicle's efficiency. The active grille shutter system functions by detecting the vehicle driving status through respective modules and sensors. Therefore when the air (which cools the underbay) is not needed, the shutter closes and a smooth airflow envelops the vehicle leading to a lower drag coefficient enabling the car to slip through the air. The actual shutter system which can be seen in Fig. 8 that show the grille shutter for the Volvo XC40 with major components such as the frame (or housing), the vanes, air guide.

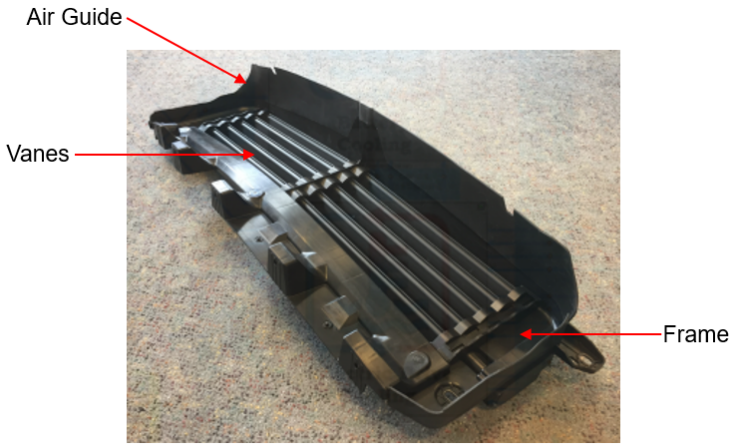

Figure 8: Active Grille Shutter used for the Volvo XC40 with major components [26]

Active grille shutters have been used for quite some time in internal combustion engine vehicles. There was quicker engine warm-up thanks to the reduction of air flow through the front end of the vehicle toward the engine compartment. There are other advantages such as lower engine noise and heat retention and quicker cabin heat-up in cold conditions. This ultimately led to entailing higher fuel efficiency, lower greenhouse gas emissions. Now for electric vehicles, this system plays an ever important role in thermal efficiency.

Electric cars are highly digital and they are most likely to include active aerodynamic components to boost vehicle range, optimize motor temperatures and battery cooling. In the case of current vehicles, it is standard among vehicle manufacturers to have both a grille and spoiler shutter. The grille shutter is located above the top crash beam and the spoiler shutter is often situated underneath the crash beam as shown in Fig. 9. Based on the market trends and engineering judgments in-house, and looking at the current BEV on the market (for instance Tesla or Nissan Leaf), the spoiler shutter is likely to be the only opening for the future Volvo BEV's while the grille would be closed. [26]

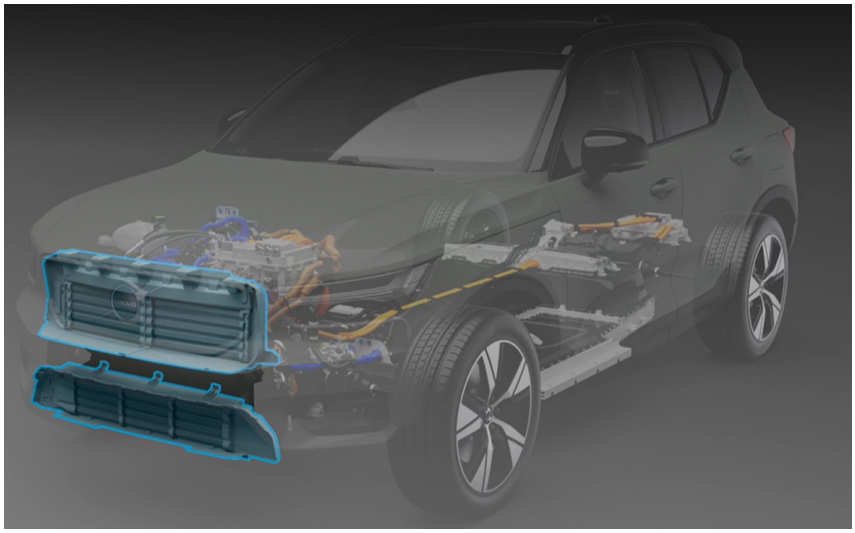

Figure 9: Active Grille Shutter location [26]

2.7 GT-SUITE

GT Suite is a 0D/1D/3D multi-physics CAE system simulation program developed by Gamma Technologies. GT-SUITE has a collection of component libraries that replicate the physics of fluid flow, thermal, mechanical, electrical, magnetic, chemical, and controls. It is widely regarded as a leader in high-level system modeling (0D/1D). GT-SUITE is also a detailed 3D modeling tool, with built-in structural and thermal 3D FEA (with in-situ meshers), 3-D multi-body dynamics with flexible bodies, and 3D CFD. These are supplemented by CAD modeling and automated model production from CAD. GT-SUITE is based on one-dimensional fluid dynamics, describing flow and heat transfer in pipework and other cooling system components.[27]

Several parallel fluid circuits, each holding a different fluid (water/glycol combination, oil, transmission fluid, air, etc.), can be represented at the same time. These circuits connect via heat exchangers, which transfer heat from one circuit to another, allowing the overall heat balance in the system to be computed.

Along with fluid flow and heat transfer capabilities, the code includes additional specialized models necessary for system analysis. The code is well suited for integrating all heat management tasks that arise throughout vehicle development. It also features a built-in vehicle simulation for calculating thermal loads under any driving cycle, as well as the flexibility required to simulate complex concepts. GT-ISE is the graphical user interface, while GT-POST is the post-processing interface [27].

2.8 Complete Vehicle Thermal Model

The Complete Vehicle Thermal Model (CVTM) is a 1-D system-level model that is used in Volvo Cars for entire vehicle thermal management in GT-Suite. The CVTM methods are modeling standards used to minimize maintenance of models, make them accessible to users other than the model creators and allow analysis-engineers to combine models to perform more complicated analysis. The areas currently working with this method are: Hybrid electric vehicle cooling, BEV Cooling, Electric Propulsion and Climate Systems. This method allows integrated thermal and flow calculations from the concept stage all through to verification. This model allows users to access different vehicle architectures in one place across battery electric vehicles and hybrid electric vehicles. The Compact Modular Architecture (CMA) for a BEV, which is a vehicle platform jointly developed by VCC and Geely is used for the study in CVTM. Sensitivity and optimization studies can be performed among the different vehicle groups to make more accurate estimations of the power consumers of a BEV. The thermal system development team at Volvo Cars is responsible for the development of this model. The user interfaces as shown in GT-ISE are displayed in Fig. 10. where the user can access the various sub-assemblies.

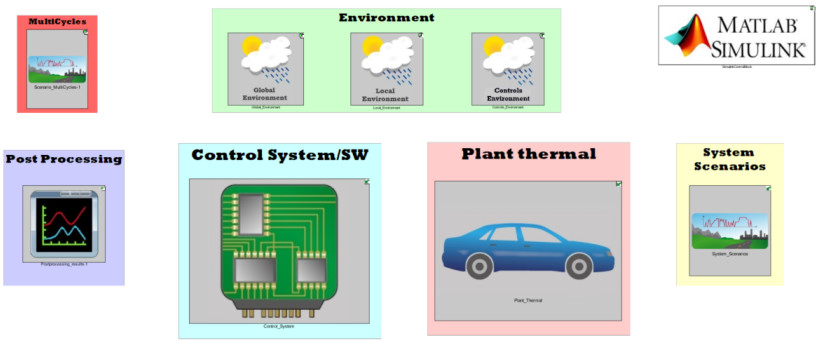

Figure 10: CVTM Interface

2.8.1 Vehicle Modelling in CVTM

The entire vehicle thermal management system is modeled in CVTM at the 1-D level. GT-ISE is used for system modeling. The primary interface of CVTM containing the sub-systems is shown in Fig. 10. consisting of the Environment which contains various environments for the model, where the ambient conditions for the vehicle can be altered. The Control System consists of the control components and the algorithm's implemented for the systems to function. The Post Processing module displays the simulation results, the System Scenario which has the signals required by all the system models as boundary conditions that are not related to control systems. The Plant Thermal is the primary sub-system containing all the modeled thermal components and the circuits. Each sub-system contains the various sub-assemblies. These sub-assemblies contain further sub-assemblies systems that are all interlinked to each other.

The primarily used sub-assemblies are the Control System and the Plant Thermal. The Control System sub-assembly contains the control logic's of the various regions of the system such as the battery, propulsion, cabin etc as shown in Fig 11.

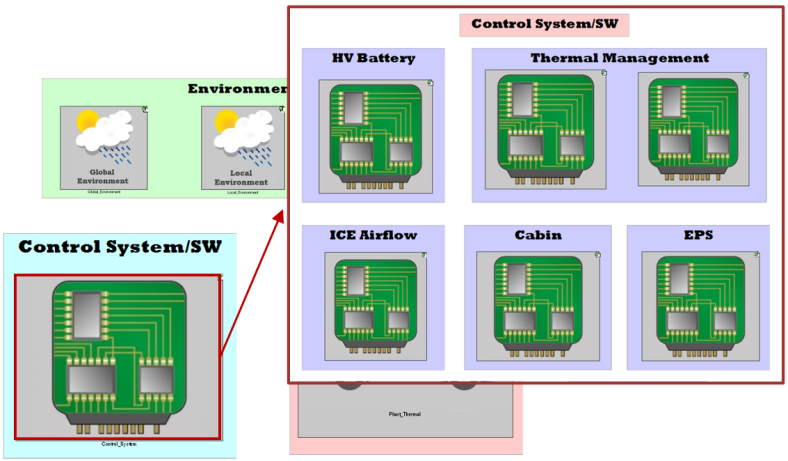

Figure 11: Control System Sub-Assembly

The Thermal Management sub-assembly is primarily used herein the study, which consists of the control logic used for cooling components such as the cooling fan, pump etc. The control system mainly consists of signals generators, receivers and other control components connected with the logic implemented by various blocks, such as the if then else blocks. The control algorithms decide the operating points of different components based on input signals and driving behavior of the vehicle. The plant thermal contains all the modeled thermal system components. CVTM is modeled for a hybrid vehicle or a BEV, therefore depending on the vehicle platform choice the analysis can be done. Hence it contains various dummy components such as engine cooling and other hybrid vehicle components in the system while choosing a BEV platform. In the plant thermal sub-assembly, the thermal management systems are further divided into vehicle regions as shown in Fig. 12 such as the climate comfort, cooling system, internal combustion engines, electric propulsion systems.

These regions contain the respective sub-assemblies such as HVAC, battery cooling, air cooling, etc which contain the 1-D model of the system. Each further sub-assembly based on the vehicle cooling regions contains components which are interlinked together with various sensors, pipes, pumps etc. The components contain data derived from external suppliers to replicate actual characteristics. Most components such as heat exchangers etc contain air flow maps or pressure maps that contain data from suppliers to model them. These components with the surrounding connections are further linked via signals to the surrounding sub-assemblies and further to the main plant thermal sub-assembly.

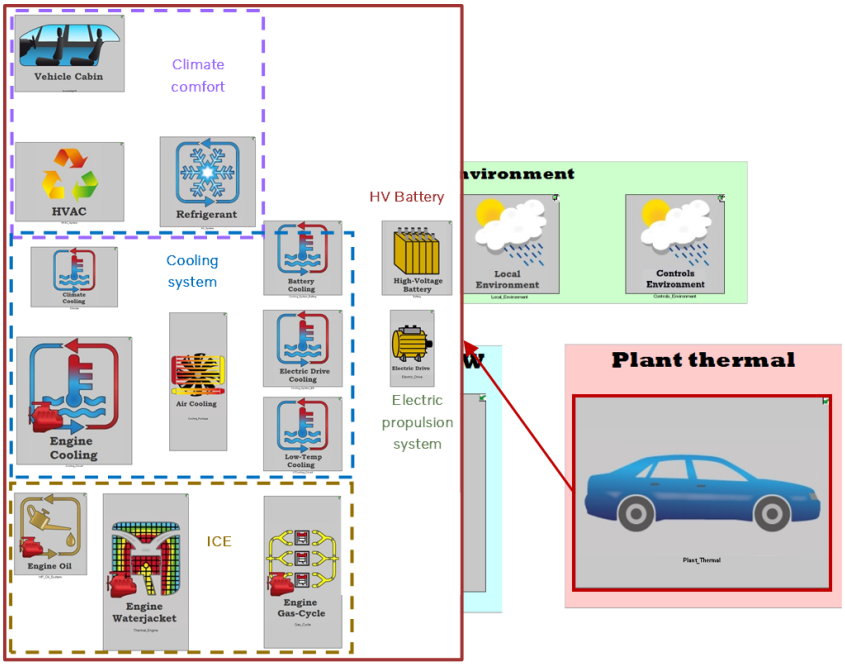

Figure 12: Plant Thermal Sub-Assembly

2.8.2 Components of Interest Control Logic in CVTM

The thermal management system consists of numerous components and only certain components of interest is taken into account for this study. They are the Compressor, Cooling fan, Electric Drive Electric Water Pump (ED EWP), and the Battery EWP when the chiller is switched on. Each component is taken from each respective sub-system of cabin cooling, air cooling, Electric drive cooling, and battery cooling. The chiller can be switched on/off in the Chiller Switch in the Controls AC tab under the Case Setup option. This is based on whether battery cooling is required for the case. All the component control logic's are indicated in the control system sub-assembly in CVTM.

For each component, a control method is implemented in GT-ISE for it to replicate as close to real component behavior at the 1-D level. The compressor operating points are derived from the compressor speed and the mass flow rate through it from a map. The map is a table containing the corresponding variables used without the data to obtain the outlet pressure for deriving the power from the compressor. The compressor speed is regulated with the help of a proportional-integral derivative controller (PID) controller. The controller takes its input from the Evaporator Air Outlet Temperature. There is a pre-conditioned setpoint value of 3°C which is the Target Evaporator Outlet Temperature. The controller calculates the error difference between the setpoint value and the actual evaporator air outlet temperature. The error is multiplied by the modes of action of either the proportional, integral, or derivative gain to regulate the RPM. The Proportional Integral (PI) mode are used here where the gain and the integral is multiplied to the error to give the desired compressor speed.

The data for the inputs of the compressor map is obtained from the supplier and based on the two values of compressor speed and mass flow rate the discharge pressure of the compressor is obtained, where the corresponding power is obtained.
The cooling fan behaviour is based on the control logic that is based on the compressor outlet pressure(P) as shown in the Table 4 below. Based on the discharge pressure, the cooling fan speed is regulated. The output is the fan Pulse Width Modulation (PWM). The fan PWM used here is the control signal used for regulating the cooling fan speed. It describes the percentage of maximum fan speed used at that instance in the vehicle.

Actions	Conditions (bar)	Output (Fan PWM)
If	P≥20	90
Elseif	P≥15 && P<20	65
Else		0

Table 4: Cooling Fan Control Logic

The formula used to derive the Cooling Fan power (F) from PWM is displayed in eqn.(4)

$$F = 0.00056 * x^3 - 0.00498 * x^2 + 0.66967 * x \tag{4}$$

where x is the PWM for the respective component and the power derived in Watts (W). The Electric Drive Electric Water Pump (ED EWP)is the next component with its logic derived from electric drive radiator coolant outlet temperature (T). The pump speeds for the coolant temperatures is shown in Table 5. The output is the Pump Speed PWM where the power is derived from for the ED EWP.

Action Descriptions	Actions	Temperature Conditions (°C)	Output ED EWP Speed (PWM)
ED Pump at 25%	If	T<35	25
ED Pump at 50%	ElseIf	T≥35 && T<45	50
ED Pump at 60%	ElseIf	T≥45 && T<50	60
ED Pump at 80%	ElseIf	T≥50 && T<54	80
ED Pump at 100%	ElseIf	T≥54	100
	Else		25

Table 5: Electric Drive Electric Water Pump Control Logic

The battery Electric Water Pump working logic is based on whether active, passive cooling, or no battery cooling is required in the thermal management system. The battery pump speed is regulated based on this. If active cooling is desired, the cooling pump speed is based on the request from Electric drive EWP for cooling. The logic for the Battery EWP is displayed below in Table 6.

Action Descriptions	Actions	EWP Speed (PWM)	Output Battery EWP Speed (PWM)
Passive Cooling Request	If	100	100
Active Cooling Request	Elseif	EWP speed request	100
No Battery Cooling	Else	EWP speed request	20

Table 6: Battery EWP Control Logic

2.8.3 Air Flow Modelling in CVTM

In the air-cooling heat exchangers section of CVTM, the mass flow rates are modelled in the thermal model. The mass flow rate for the heat exchangers i.e the condenser and radiator in CVTM is modelled from an air flow map which is a table that contains certain fan Pulse Width Modulation (PWM) and vehicle speed data points derived from experimental data or previously simulated 3D-CFD data from the department. A single look-up table template is used containing an XYZ template map from GT-SUITE, where the mass flow rate (Z) is derived from the vehicle speed (X) and fan PWM (Y) as shown in Fig.13 containing dummy values. The remaining values between the available data points are interpolated by the template to give the desired mass flow values. The mass flow rate value is found from this table to be input into the heat exchangers which affects the thermal management system.

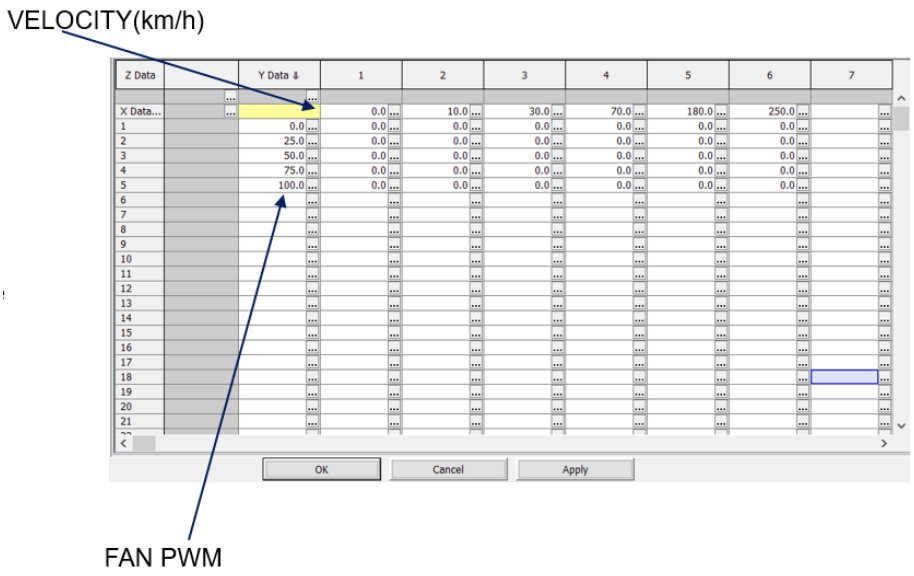

Figure 13: Air-flow map with dummy values

3 Methodology

3.1 Sensitivity Analysis

Thermal systems are usually a compromise between multiple components operating at their limits. A sensitivity analysis has to be performed to understand how the operating points of these components can be varied to benefit the overall energy efficiency of the vehicle. This would give an idea of the model behavior as well. The complete vehicle thermal model (CVTM) is used, which is an interlinked model for the various control systems in the car for the thermal management components. The controls in the thermal model mimic the behavior of the real control system in the car.

Initial sensitivity studies under different operating conditions are performed on this model to see the effect of the change in power consumption of the components of interest in the thermal management system. The velocity of the vehicle is indicated by a drive cycle. As there are different instances of driving scenarios such as city,highway driving etc. A driving cycle is a series of data points representing the speed of a vehicle versus time to test vehicle's performance before they enter the market.[28] Driving cycles are used by different authorities to assess the performance of vehicles in various ways, as for instance fuel consumption, electric vehicle autonomy and polluting emissions. The drive cycle used here is the Worldwide harmonized Light vehicles Test Cycles (WLTC)[29] which is used in Europe since 2017 for testing vehicles. The WLTC drive cycle mimics real-world driving conditions at various stages such as driving at high speed or stopping the vehicle in some instances. The standard WLTC Drive cycle, which is a speed (km/h) vs time plot (s) as displayed Fig.14.

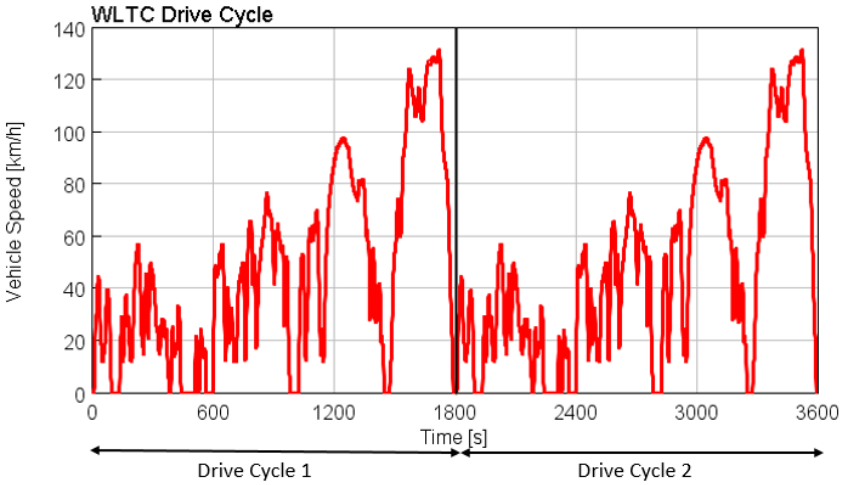

Figure 14: 2 x WLTC Drive Cycles

Two identical drive cycles each of 1800 seconds are taken into account, hence the car is simulated for 3600 seconds drive time.

The best practice guidelines for 1-D simulations is to use two drive cycles, which are used to observe the effects of the performed variations on the vehicle along time. One drive cycle may not be sufficient to study the variations due to the vehicle components taking time initially to get up and running. Hence, simulating another drive cycle allows to see variations on the components for a longer period of time to gather the data to see the effects for two drive cycles. The vehicle is simulated for a cool-down case, where the vehicle is at high temperature and brought down to a low temperature. The grille shutter is completely open for these studies and the heaters are switched off. The trends of the component parameters across the drive cycle and final power consumption are noted for each component when the changes are made.

Absolute integral values of power for the entire simulation are derived using the integral mathematical function in GT-ISE which integrates the values along the time period in order to derive a single value. Report files are created with the required parameters in GT-POST for post-processing. The most relevant parameters related to the components of interest are plotted in the next result section. The studies are performed to see the effect on the overall power consumption of the thermal management system. The various sensitivity studies that will be performed below are-

1. 3.1.1: Mass Flow Rate Change Study
2. 3.1.2: Cooling Fan Speed Change Study
3. 3.1.3: Ambient Temperature and Battery Cooling Change Study

3.1.1 Mass Flow Rate Change Study

This is the first study where the mass flow rate through the vehicle is varied to see its effect on the system components and the power consumption across four cases. A base case of the ambient temperature of 35°C, with an initial cabin temperature of 38°C is set to cool down the vehicle to a cabin temperature of 21°C. This case is the default cool down case in CVTM, with the 35°C temperature being an optimum temperature for the case not being too cool or very warm. Four cases of mass flow rate variation from the base case are performed. The flow rate is decreased 5%, 10% and increased 5%, 10% from the base case. These changes were considered effective enough to see variations in the thermal model component results. The mass flow change is implemented by changing the air flow maps as explained in the air flow modelling section in the Theory. The radiator and the condenser air flow maps values are added/reduced by the desired percentages for each case. The battery cooling is switched off hence components such as the chiller are not active for simplicity. The initial conditions discussed above are shown in Table 7 remain the same in all varied cases, with only the airflow values changing. The simulation is run and results are viewed in GT-POST. The varied mass flow rate results are compared with the base case.

Initial Conditions	Value
Ambient Temperature	35°C
Cabin Temperature	38°C
Grille Shutter	90°(Fully open)
Velocity	2 X WLTC Drive Cycle

Table 7: Initial Conditions for the Mass Flow Rate change study cases

3.1.2 Cooling Fan Speed Change Study

For this study, the cooling fan speed is increased to study its effect on the system and the overall power consumption. The control logic of the fan is changed for this. This can be changed in the Control System sub-assembly and further in the Thermal Management Vehicle Control Unit (VCU) sub-assembly. The current programmed control logic of the cooling fan for the base case run in the previous Mass Flow rate section study runs at 65 PWM. This speed is by default for the corresponding compressor pressure output as shown in the control logic of the fan in the previous theory section. With the cooling fan limited to 80 PWM in CVTM, another case is run for the fan speed is increased from default 65 to 75 PWM to observe changes with the same driving conditions. In the VCU sub-assembly under the cooling pack fan-control region, the cooling fan speed is a function of the compressor outlet pressure and this is changed from 65 to 75 for the same outlet pressure. The increased cooling fan speed case therefore uses the same initial conditions as the base case, only with the control logic changed to increase the fan speed. The same initial conditions for both cases are shown in Table 8. Battery cooling is ignored for this study. The cases are run and results viewed in GT-POST.

Initial Conditions	Value
Ambient Temperature	35°C
Cabin Temperature	38°C
Grille Shutter	90°(Fully open)
Velocity	2 X WLTC Drive Cycle

Table 8: Initial Conditions for the Cooling Fan Change Study cases

3.1.3 Ambient Temperature and Battery Cooling Change Study

For this study, the ambient temperature and initial battery temperature are changed to observe variations in the thermal management system components. The battery cooling is turned on. A higher ambient temperature is taken to add to the cooling load to be brought down to a lower temperature. Totally four cases are taken into account for this study. An initial 35°C ambient temperature with 38°C cabin temperature is used with two cases of initial battery temperatures of 38°C and 46°C. Other cases for a higher initial ambient temperature of 46°C is also taken with 46°C cabin temperature with two cases of 38°C and 46°C initial battery temperatures.

The combined ambient and battery cooling four cases are displayed in Table 9. The cabin temperatures for all cases are brought down to target values of 21°C and the battery temperatures are brought down to 28°C. These target temperature values are decided by the climate team at VCC which are standard values for cool down vehicle thermal management related studies. The two WLTC drive cycles are used with the grille shutters remaining fully open.

Cases	Ambient Temp. (°C)	Cabin Temp. (°C)	Battery Temp. (°C)
35_38	35	38	38
35_46	35	38	46
46_38	46	46	38
46_46	46	46	46

Table 9: Ambient temperature, Cabin and Battery cooling change cases

3.2 Improvement of the thermal model with AGS

3.2.1 AGS Implementation

The Active Grille Shutter (AGS) needed to be integrated into the complete vehicle thermal model in GT suite for the particular vehicle platform to vary the grille shutters, just as how it is implemented in the vehicle. The initial CVTM is modeled in a way that the grille shutter to be the fully open at one angle. This meant that the model could only be simulated in the fully open grille shutter state for the entire time period. For the AGS to be implemented, multiple shutter angles need to be implemented so that the grille shutter angles vary in the model along the drive cycle depending on the cooling air demand and vehicle speed. In the Plant Thermal sub-system, the air cooling assembly contains the radiator and condenser where the circuit is altered. The thermal model which consists of an air flow map that contained a single look-up table as shown in Fig.13 for one shutter angle of 90°. The air flow map data is derived from 3D CFD. The heat exchanger picks the mass flow value from the air flow map. The process for deriving the airflow from the look up table is explained in the previous Airflow Modelling section in Theory. The output signal goes directly into the next block which leads to the heat exchanger. The initial condenser sub-assembly configuration containing one air flow map in CVTM is observed in Fig 15. To implement AGS multiple look-up tables would need to implemented for all the shutter angles. This is implemented further.

Data to derive the mass flow rates was only available for five shutter angles, which are 0°,9°,20°,45°,90° from existing 3D-CFD data simulated by the department. The rest of the mass flow rates for other shutter angles between the above five corresponding shutter angles needed to be interpolated in the model.

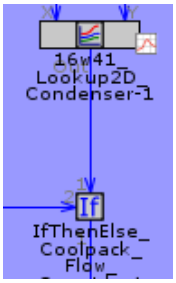

Figure 15: Initial Condenser Configuration with One Air Flow Map

For this to work, the interpolator template is used. This template produces an output signal by comparing the control signal to the Look-up Array values which are either defined by the user inside the Arrays folder or by external signals.[27]. The look-up array defined here are the five air-flow maps. Each look up table contains one air-flow map representing one of the five angles. The interpolator template receives the signal for the desired shutter angle from the case setup where the shutter angles degree vs time data is input and looks for the angle value from the given air-flow maps. The template interpolates linearly in the forward direction, therefore the search for the desired flow rate will start with the first air-flow map. Then an output signal is produced which contains the desired mass flow rate that is used as an input into the heat exchangers. The implemented sub-system is shown in the Fig. 16 for the condenser with the five lookup tables containing the airflow maps and the interpolator block connection. The same sub-system will be implemented for the electric-drive radiator as well.

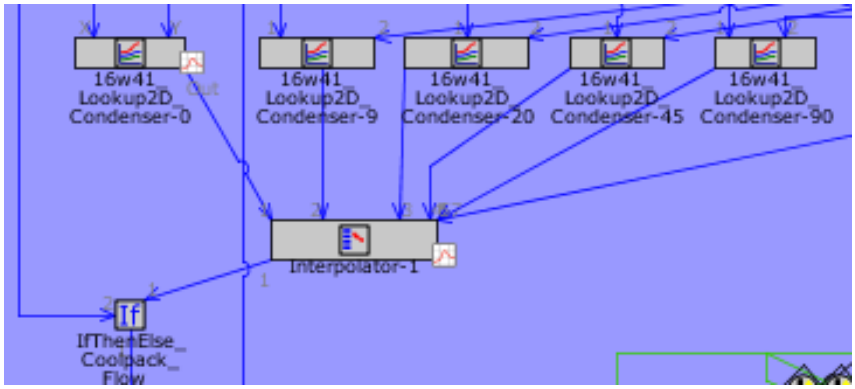

Figure 16: Implemented AGS Condenser Configuration with interpolator

On implementation of the control sub-assembly, an integration check is performed to see the working. The components of interest are observed to see variations based on the grille shutter opening and closing. The output signal from the interpolator block for the particular shutter angle is verified manually to derive the exact mass flow rate value into the heat exchangers.

3.2.2 Cooling Fan Speed Control Block Implementation

The AGS system control sub-assembly is implemented in the model in the previous AGS implementation section. The transient shutter angles is input in the shutter angles variable in CVTM. The shutter angles for the AGS to be input in the model which is derived from experimental data for the initial optimizations are shown below in Fig.17 along with how the angles vary with the varying velocity in the drive cycle. These shutter angles are for the same ambient temperature and drive cycle as from the data in the tests. Battery cooling is not taken into account for simplicity and it was also observed from the sensitivity studies that the battery cooling did not have any significant effect from the variation of shutter angles apart from being an added load case. The same components of interest are observed as the sensitivity studies with the compressor, cooling fan and electric drive are taken into account.

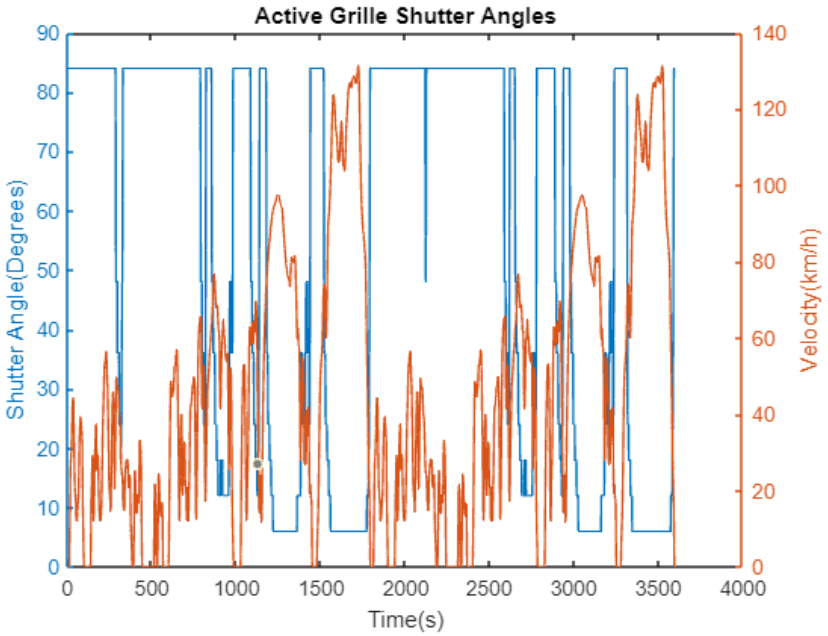

Figure 17: Active Grille Shutter Angles

The grille shutter angles are input in the case setup and the model is simulated with the initial conditions shown in Table 10.

Initial Conditions	Value
Ambient Temperature	35°C
Cabin Temperature	38°C
Grille Shutter Angle	Varying Transient Angles
Velocity	2 X WLTC Drive Cycle

Table 10: Initial Conditions Optimization

The vehicle is simulated and on observing the results, an inaccuracy for the cooling fan PWM is noticed. It is observed that the cooling fan start initiation needed to be also regulated based on the AGS angles input into the model. The cooling fan Pulse Width Modulation (PWM) default fan logic result is shown below in Fig 18. Instances are observed in this plot such as for eg. at the 400-second mark when the grille shutter closes from fully open state, the fan is still running around 70 PWM. The cooling fan is expected to switch on only when the grille shutters are fully open, hence when the shutters are closed/partially open it is expected to switch off. One of the issues is that if the cooling fan runs even with the grille shutters closed, the recirculated hot leakage air from the fan flows on the condenser which is not beneficial for the thermal management system [30].

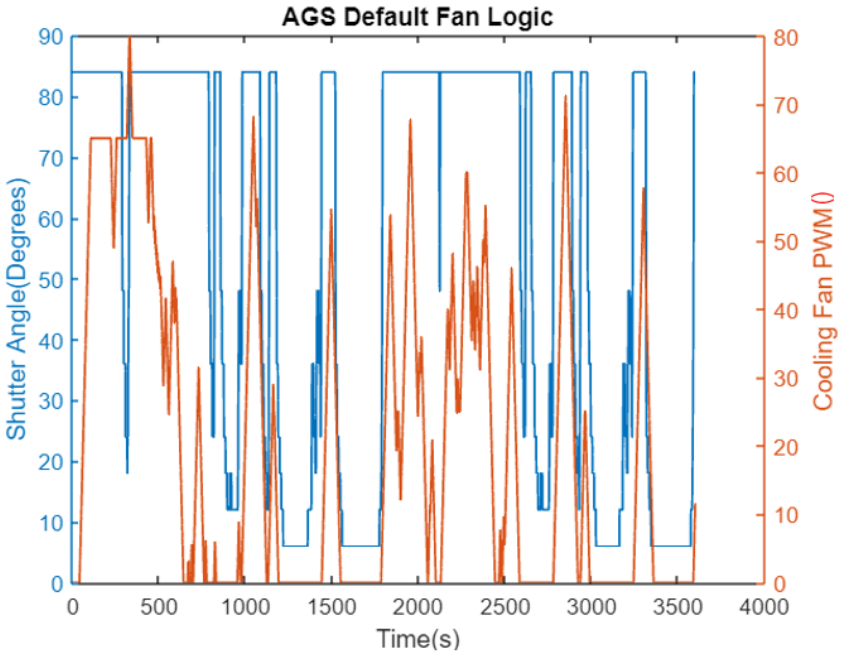

Figure 18: AGS Default fan logic PWM

This needed to be corrected in the control logic of the fan. The control system subassembly of the thermal model contains the cooling fan control section, where the fan control logic is implemented. After the fan speed is regulated by the compressor as indicated in the previous section, an extra control block would need to be added to link the shutter angles to the fan control logic.
This control block contains an if-else logic that regulates the cooling PWM to zero when the shutters are closing. The cooling fan speed translates to the cooling fan PWM. A signal from the grille shutter angles is brought into this block and the control logic is implemented. The logic states that if the shutter angle is less than 84 degrees i.e the fully open case from the test data the fan speed is regulated to zero, else the fan speed signal continues to go normally to the send block. This would result in the cooling fan start and stop, also taking the implemented AGS into account. The if-else block is implemented and run for the same initial conditions to see the changes.

3.2.3 Manual Fan Control Implementation

The results of the mass flow rate through the heat exchangers are also observed throughout the entire simulation. For the existing model, a discrepancy is observed in the mass flow rate through the condenser. The flow rate drops almost to 0 (kg/s) in several instances in the drive cycle as shown in Fig.19. This is seen that at points for eg. such as at the 1000 s, 1500 s mark in the plot the mass flow rate drops to zero. This should not be the case as there has to be airflow in the vehicle, even when the vehicle stops to cool the thermal management system components.

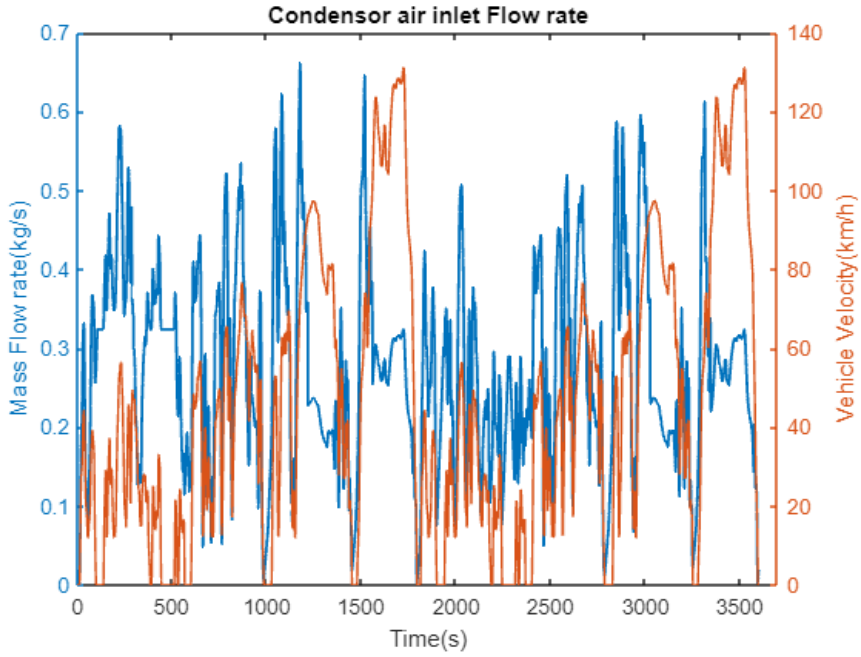

Figure 19: Default Logic Mass flow rate condenser

According to the cooling fan working, the fan needs to start when the vehicle velocity drops to zero. Hence, the cooling fan needs to start running to initiate the airflow flow into the vehicle to keep the components cool. This is not being achieved by the current model where instances of mass flow rate dropping to zero are observed in many instances in the plot. On investigation, it came down to the fan controller delay in the control logic.

A solution is to include the fan PWM from tests for the same driving and initial conditions into the model to force the cooling fan to run at the correct speed so that the desired correct mass flow rates through the heat exchangers could be achieved. Test data for 35°C ambient temperature and 40°C cabin temperature were available. This would force the fan to run at the desired correct speed with manual fan control implementation in the model. The manually implemented fan PWM is shown in Fig. 20 as compared with the default PWM. It is seen that the PWM from GT-ISE seems to over-predict the power compared to the test values from the car with much higher values peaking and bottoming to very low values. The fan controller configuration is also changed from Default to Manual and the fan PWM from tests is input into CVTM.

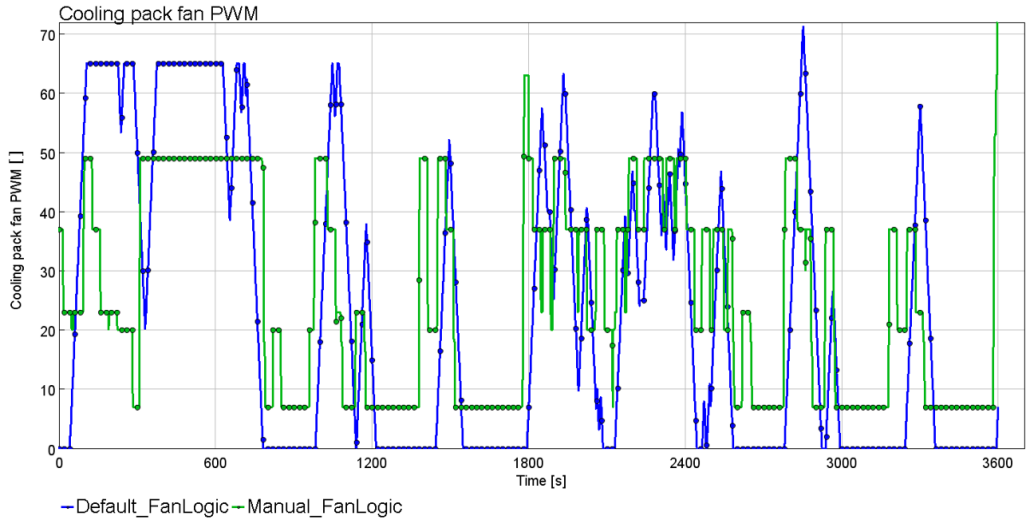

Figure 20: Fan PWM

The simulation is then run for the initial conditions below in Table 11. The conditions used are based on available test data to input for the cooling fan in GT-Suite, in order for the manual fan control to be implemented. The vehicle is simulated for 3600 seconds.

Initial Conditions	Value
Ambient Temperature	35°C
Cabin Temperature	40°C
Grille Shutter Angle	Varying Transient Angles
Velocity	2 X WLTC Drive Cycle

Table 11: Initial Conditions Manual PWM

3.2.4 Improved Fan and Shutter Control Implementation

The current control logic involves the cooling fan to be manually implemented from the fan data from tests and the active grille shutters data to be fixed irrespective of the mass flow rate through the heat exchangers. This is not feasible for various boundary conditions as seen in the previous Manual Fan Control Section, data from tests would need to be readily available for each setup. Also, a better method needed to be implemented for the grille shutters and cooling fan to be inter-dependent in the system. This implementation is done to derive the mass flow rate through the heat exchangers in the model just like a real-world vehicle would, rather than just be based on compressor data in the previous logic. A matrix is plotted with airflow values for certain fan and shutter combinations derived from existing 3D-CFD data from the department. This matrix containing air flow values for fan and shutter combination is split into two plots as shown in Fig. 21.

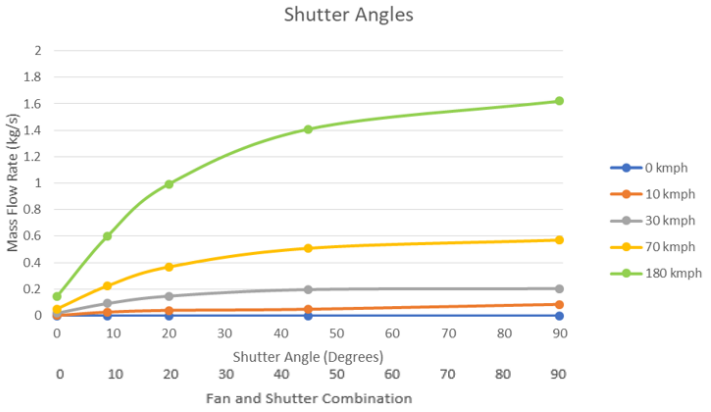

(a) Shutter Angles Variation

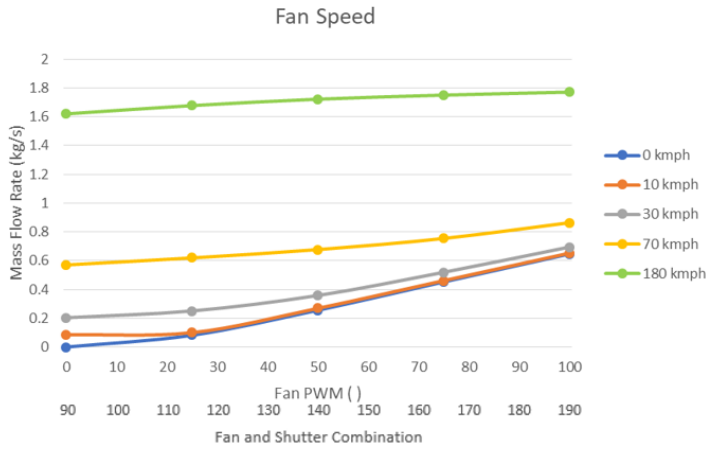

(b) Fan Speed Variation

Figure 21: Fan and Shutter Combination Matrix

The plot (a) contains the mass flow rate for varying shutter angles and the plot (b) contains the varying fan speed flow rate values. Five vehicle speeds are plotted at 0, 10, 30, 70, 180 kmph in both plots.

The plot (a) is defined such that the X-axis corresponds to varying grille shutter angle values from 0-90° with no cooling fan, as the fan switches only when the grille shutter is fully open at 90°. The fan is at zero PWM hence the combination of fan and shutter on the secondary X-axis is the same as the first x-axis for shutter angles. The Y-axis shows the mass flow rate values. The plot (b) shows the fan speed values (PWM) on the first X-axis with the constant grille shutter angle of a fully open angle i.e 90° and the mass flow rates on the Y-axis. The X-axis contains fan PWM values from 0 to 100 PWM and Y-axis containing mass flow rates indicating switching on of the fan. The secondary X-axis containing fan and shutter combination starting at 90 when the shutter is fully open constantly for the entire plot. The fan PWM values are added up to the fully open shutter angle from 90 up to 190 on the X-axis. The maximum value of the plot is 190 with a shutter angle of 90° and a fan PWM value of 100. This is the basis of the plots.

This combined matrix is integrated into a MATLAB code which on the input of the desired mass flow rate values picks the values from the plot that gives grille shutter and fan PWM values. The code connects the mass flow rate to the fan and shutter values in the matrix at different velocities along with the plot. The outputs are fan PWM values and grille shutter angles. The values in between the data points from 3D-CFD are linearly interpolated in the code to give the desired outputs. These grille shutters and fan PWM values will be entered into the case setup of CVTM and simulated. Manual fan control will continue to be implemented with the fan PWM from the code. Based on the values input from the code into GT-ISE the cooling fan and grille shutters will be derived based on the mass flow rate. The vehicle will now be simulated based on this updated method, where the mass flow rate is derived in the model with the fan and AGS varying to bring in the air flow. All further simulations are run using this method.

3.3 Impact of Additional Mass Flow Rate on Energy Balance Study

The implementation of Active Grille Shutters (AGS) is expected to improve vehicle aerodynamics. This would translate to energy consumption savings by reducing the aerodynamic drag. Hence it is vital to see the effects of the aerodynamics of AGS on the overall power consumption of the thermal management system. It is observed from the mass flow studies, that additional mass flow rate leads to power savings however the effect of the aerodynamic drag derived due to the implementation of AGS was not taken into account. With the introduction of the energy consumption due to operating AGS on the system, the entire power consumption with the energy consumption due to opening of shutters is added and investigated when increasing the mass flow rate.

The average mass flow rate as observed in the plot Fig. 19 is around 0.3 kg/s. For the further studies involved, the mass flow rates are kept constant in the entire drive cycles of 3600 seconds for simplicity and to understand the limits of the thermal management system for a particular mass flow rate. The constant mass flow rate for each case is started at 0.3 kg/s and is increased in intervals of 0.05 kg/s until the combination of the shutter opening and maximum fan speed is unable to provide the rquired mass flow request at all vehicle speeds. The maximum PWM in CVTM is 80 PWM where the fan works at 80% of maximum speed. On increasing the mass flow rate for each case and observing values derived from the code, it is observed that at 0.5 kg/s, the fan PWM limits set by the model are reached. Therefore the five cases are taken from 0.3 up till 0.5 kg/s. The five cases are 0.3, 0.35, 0.4 ,0.45, 0.5 kg/s of constant mass flow rate. The mass flow values are entered into the code implemented before, where fan PWM and grille shutter angles are derived. Based on these two inputs the desired mass flow rate through the model is derived. Manual fan control is implemented where the fan PWM is input for each model and the five simulations are run with a constant mass flow rate throughout the two drive cycles.

The components of interest will remain the same with the compressor, cooling fan and electric drive electric water pump. The ambient temperature of 35°C is taken with 40°C cabin temperature. No battery cooling is taken into account. Absolute power levels in KiloWatt Hours (kWh) are calculated in GT-ISE using the integral mathematical function, which integrates the data over the time period. The initial conditions are displayed below in Table 12:

Initial Conditions	Value
Ambient Temperature	35°C
Cabin Temperature	40°C
Initial Battery Temperature	27°C
Grille Shutter	Varying Grille Shutters
Velocity	2 X WLTC Drive Cycle

Table 12: Initial Conditions used for Energy balance studies

The energy consumption of the active grille shutters opening is to be calculated in this instance. This is calculated based on the grille shutter angles. The Coefficient of Drag and Area (CdA) values for the vehicle are available from tests for each shutter angle for a velocity of 140 kmph. The vehicle used for deriving these values was the Polestar 2. The vehicle CdA values for 16 shutter angles are obtained from a fully closed-angle i.e 0° to fully open shutter angle which is 90°. The difference (ΔCdA) is taken between each corresponding shutter angle CdA and the fully closed shutter angle CdA to take just the change in opening the shutters. Hence the ΔCdA is taken, which is the difference to solely take the effect of opening the shutters rather than the absolute drag values of the vehicle. The rest of the shutter angles for the ΔCdA values in between are linearly interpolated between the available 16 shutter angles. This interpolated ΔCdA is obtained using the interp1 function in MATLAB which is used for 1-D data interpolation.

The shutter angles for the corresponding case are obtained for the entire drive cycle from the code. For each shutter angle, the ΔCdA is derived. So the values are obtained for the entire drive cycle. Based on these values the Power ($P_{Shutter}$) is calculated using the equation:

$$P_{Shutter} = \frac{1}{2}\rho_{air} CdA \Delta V^3$$

Where ρ_{air} is the density of ambient air and V is the vehicle velocity along the drive cycle. The power is hence derived for opening the shutters along the drive cycle. A factor is also used to take into account the transmission losses in the electric drivetrain. Hence the power is increased by 35%, the value based on in-house data.

4 Results

4.1 Sensitivity Analysis Results

4.1.1 Mass Flow Rate Change Studies

The mass flow rate is varied, with an increase and decrease across the four cases. The trends are observed across the plots component-wise for the 10% increase in flow rate and the 10% decrease in flow rate along with the base case for comparison. The 5% increase and 5% decrease in flow rate cases plots will not be shown but absolute values will be taken into the account at the end of the study. The first drive cycle is from 0-1800 seconds and the second from 1800-3600 seconds. The first component of interest is the compressor. The compressor outlet pressure is the most relevant parameter here providing the logic for the cooling fan, and governs the compressor power is plotted against time as shown in Fig.22.

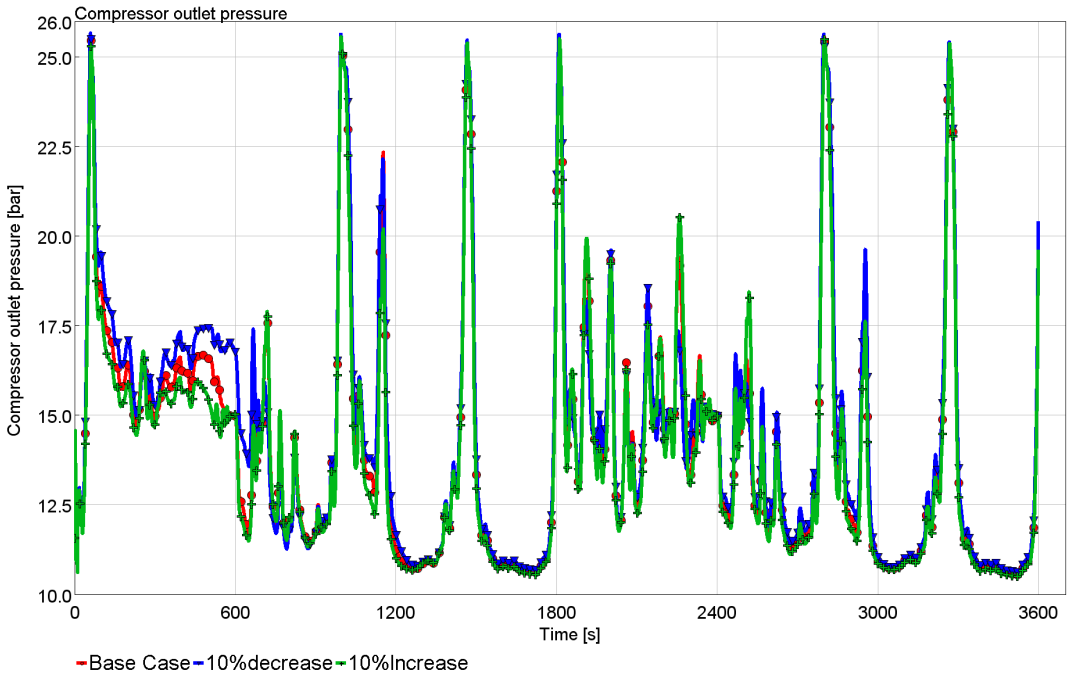

Figure 22: Compressor Outlet Pressure

The compressor outlet pressure for all cases show peaks immediately to about 25 bar, which is the set limit and then drops initially in the first 1000 seconds of the first drive cycle. This is followed by the pressure peaking and bottoming to low pressures at certain points along the drive cycle after that. Along with the three cases, the trends show the largest differences before the drop in pressure around the 500-second mark in the first drive cycle and then show similar pressure values in the rest of the drive cycles. Predominantly among the three cases, the higher pressure trends along the drive cycle are observed in the case with the 10% decrease in mass flow and the lower pressures by the 10% increase in flow case. The cooling fan is taken into account next where the fan power against time is plotted in Fig. 23.

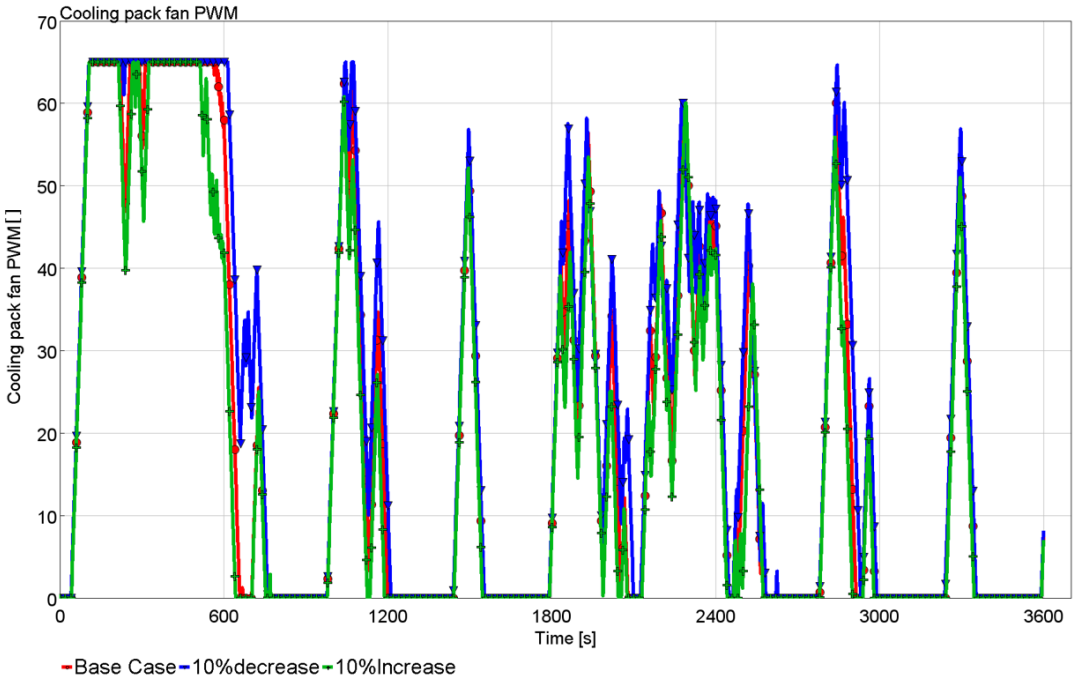

Figure 23: Cooling Fan Power

The cooling fan power trend displays that the fan is constantly high at the beginning of the first drive cycle and then switches off for some time. It then turns on and peaks followed by switching off again. A similar trend is followed in the second drive cycle after the 1800 s mark. It is observed in the second drive cycle when the fan turns on and peaks initially for a larger time period between 1800 to 2400 seconds. The trends show that the cooling fan power stays at high power of around 65 PWM initially for the longest time duration for the 10% decrease case, as compared to the other two cases before dropping. For the 10% increase case, the power drops initially the quickest followed by other cases which take more time to drop before switching on again. The 10% decrease case also peaks to higher values predominantly in the plot, followed by the base and then 10% increase case showing the least values along the time period.

The Electric drive radiator is the next component taken into account. The Electric drive radiator coolant outlet temperature vs time is plotted in Fig.24. The electric drive EWP power which gets its logic from the ED coolant radiator outlet temperature is also plotted against time is shown in Fig.25.

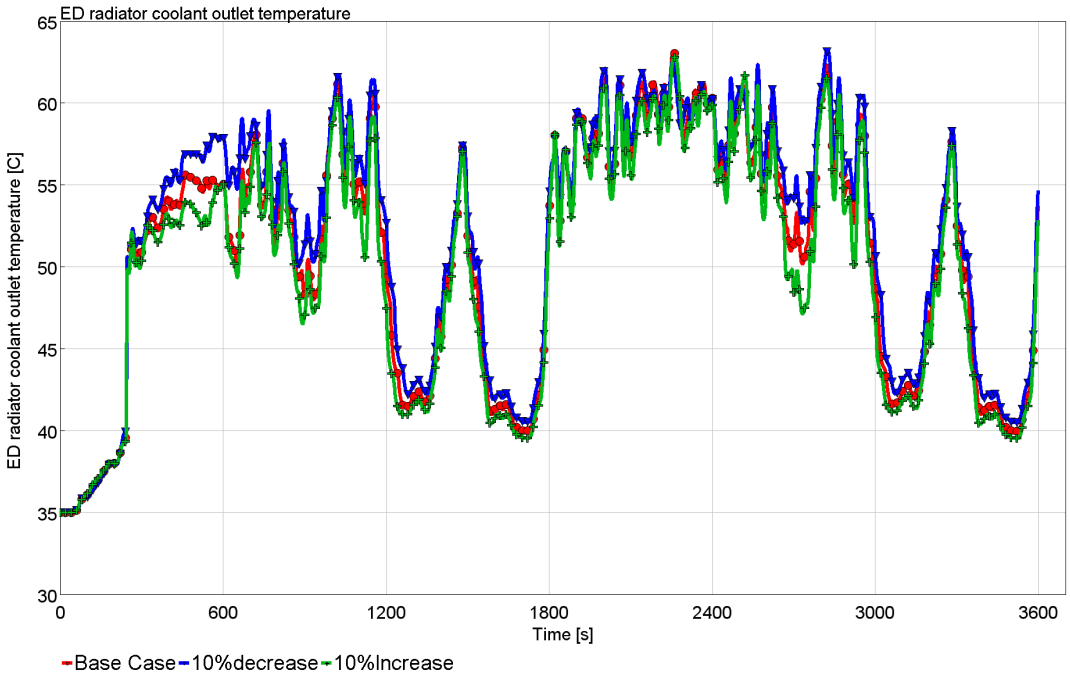

Figure 24: ED Coolant Radiator Outlet Temperature

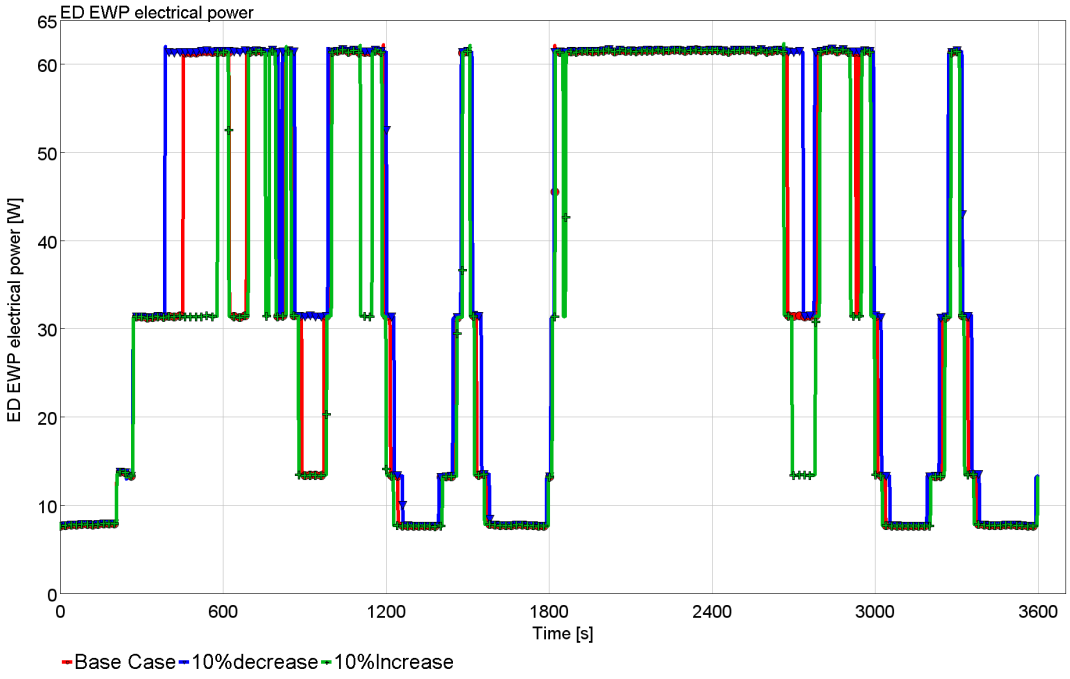

Figure 25: ED Electric Water Pump Power

The coolant temperature plot shows high-temperature values initially at the first half of both the drive cycles followed by the peaks and lows. At the second drive cycle, higher temperature values are observed averaging about 60°C. Similar trends with the rest of the components indicate that the higher coolant outlet temperature is shown by the most decreased flow rate i.e the case with the 10% decrease and the lower temperature trends is shown by the most increased flow rate i.e 10% increase. The EWP pump power peaks to about the maximum power of around 60W in the beginning first half of the drive cycle, bottoms down, and peaks again. The second drive cycle shows the pump is at maximum power constantly followed by the same trend as the first drive cycle. Similar trends to the electric drive radiator coolant outlet temperature shown in Fig 24is observed for the EWP too. The maximum pump power is used majorly for the case with the most decreased flow rate which is the 10% decrease case. For the case with the 10% flow rate increase the power drastically decreases at some points, like at 2800 seconds. The cabin temperature near the head of the left occupant is plotted against time in Fig.26.

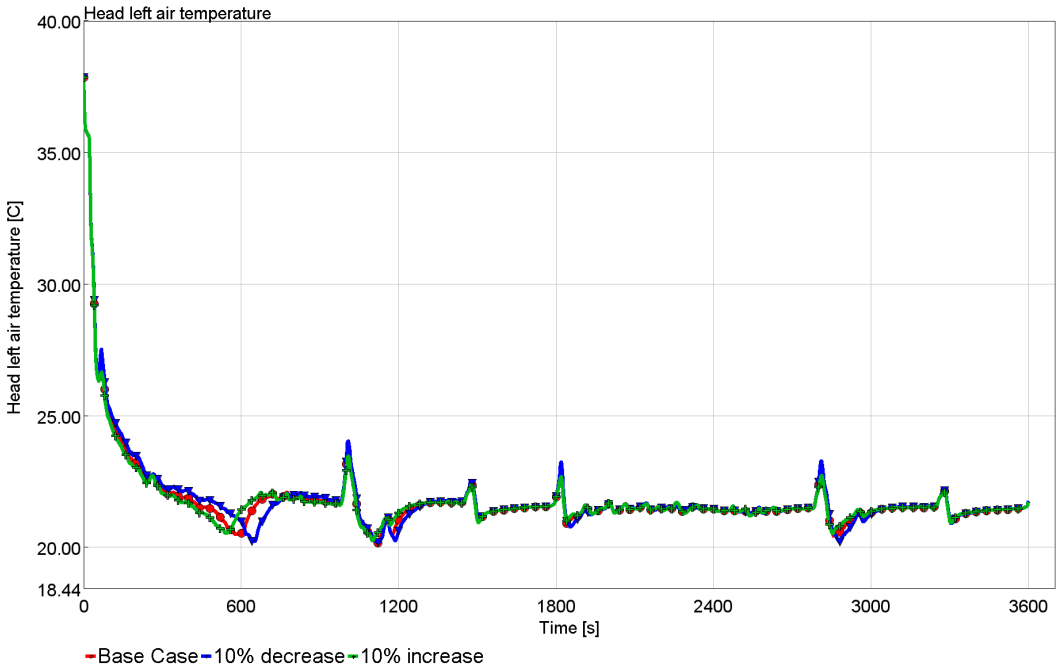

Figure 26: Cabin Temperature(Head Left)

The cabin temperature shows dropping from 38°C to the target temperature of 22°C. Among the cases, the 10% increase flow rate drops the quickest, followed by the base case and then the 10% decrease case. Instantaneous temperature changes occur along the drive cycle but all the cases mostly stabilize after the 1000 second mark. The general trends of the plots of all the components above show that the 10% decrease in mass flow has the highest values in all the plots followed by the base case and the lowest values are displayed by the 10% increase in the mass flow rate case. The power consumption of each component is derived from these components along with the base case as shown in Table 13 including the 5% increase and 5% decrease flow rates.

Case	Compressor (kWh)	Cooling Fan (kWh)	ED EWP (kWh)	Total (kWh)	Percentage Difference from base
Base	1.692	0.039	0.036	1.767	-
10% increase	1.640	0.033	0.033	1.707	-3.45%
5% increase	1.665	0.035	0.035	1.735	-1.81%
5% decrease	1.719	0.042	0.036	1.799	1.81%
10% decrease	1.754	0.045	0.039	1.838	4.08%

Table 13: Integral Component-wise and Total Power Mass Flow Rate Studies

Total Power Consumption is derived from the compressor, cooling fan and ED EWP power using the integral function and added up. The compressor shows the most power consumption compared to the rest of the components whereas the cooling fan and pump consume less power. The 10% increase case shows the least power consumption with a result of 3.45 % decrease in power. The 10% decrease case shows the most power consumption with a result of 4.08 % increase in power. The table shows almost an equal interval of percentage change of power consumption with an equal variation of mass flow rate.

4.1.2 Cooling Fan Speed Change Study

The general component behavior plots in the study follow the same trends as the mass flow rate study. The fan speed is increased to 75 PWM which is the 35_75 case and the various components are analyzed compared to the base case which is at 65 PWM speed is the 35_65 case. Similar to the mass flow study the compressor is taken first with the outlet pressure analyzed. The outlet pressure vs time is plotted in Fig. 27.

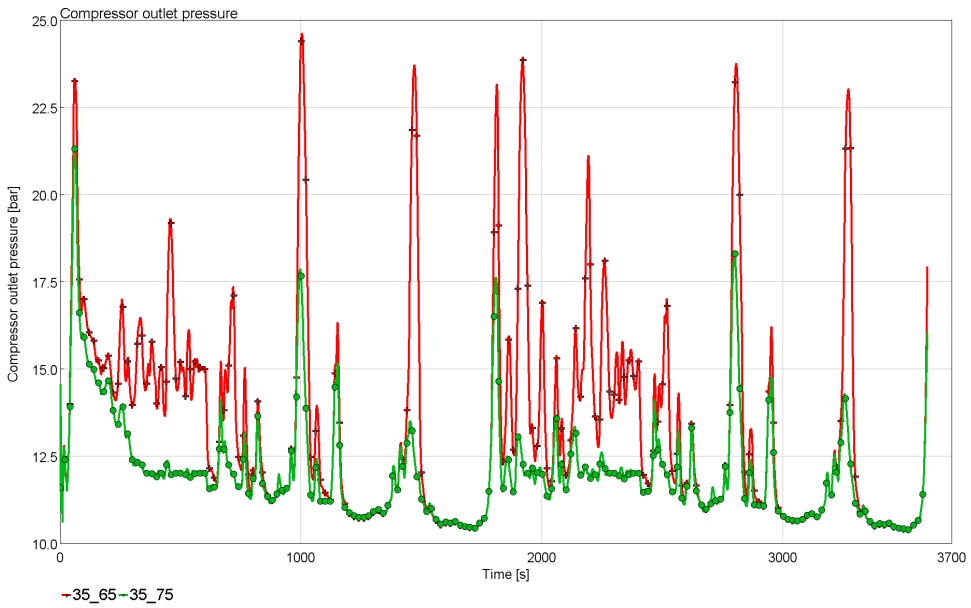

Figure 27: Compressor Pressure

Post the initial peak of high pressure in the first 100 seconds, the 35_75 case gives persistently low pressure values below 12.5 bar. Beyond the first half of the drive cycle the pressure peaks and bottom, with the 35_75 case peaking to relatively less pressure values. The same trend as the first drive cycle is followed for the second too, although the compressor pressure peaks to a maximum of about 17.5 bar. The cooling fan power is observed next as shown in Fig. 28.

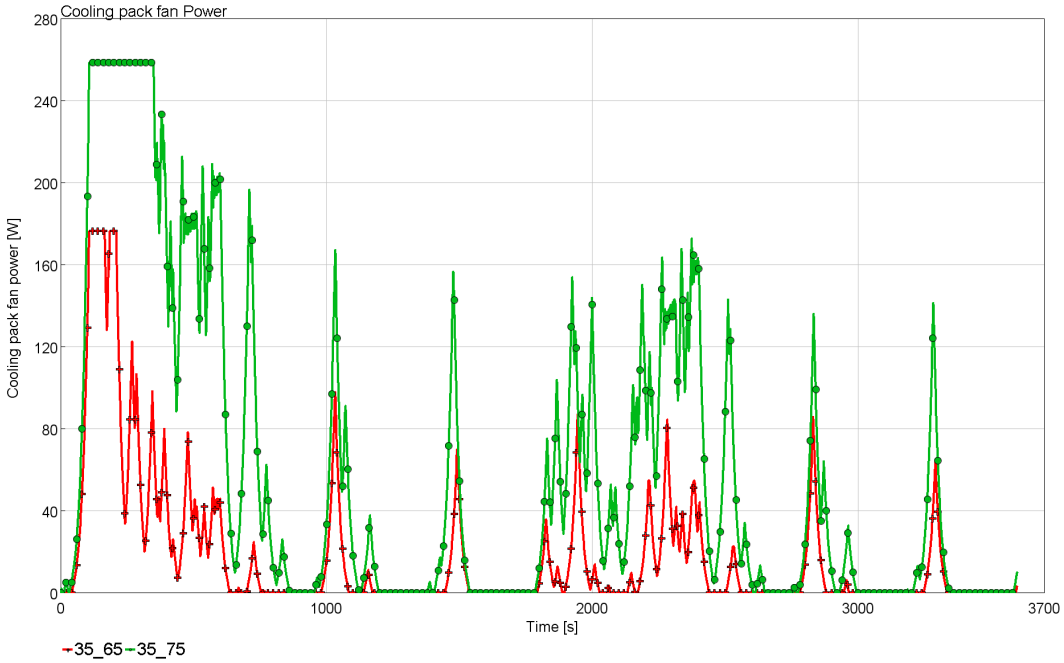

Figure 28: Cooling Fan Power

The cooling fan power displays high power in the initial stages of the drive cycle and lower power at the end of each cycle similar to the compressor. The 35_75 does not work at maximum power at any instance of the drive cycles. The trends for both cases are similar although different scales are observed. For the 35_75 case, the cooling fan shows significantly more fan power in the first drive cycle half than the 35_65 case. Further increase in power is seen in the peaks along the drive cycle. The electric drive is next accounted for with the ED radiator coolant temperature parameter displayed which also determines ED EWP power against time plot as shown in in Fig. 29 and Fig. 30.

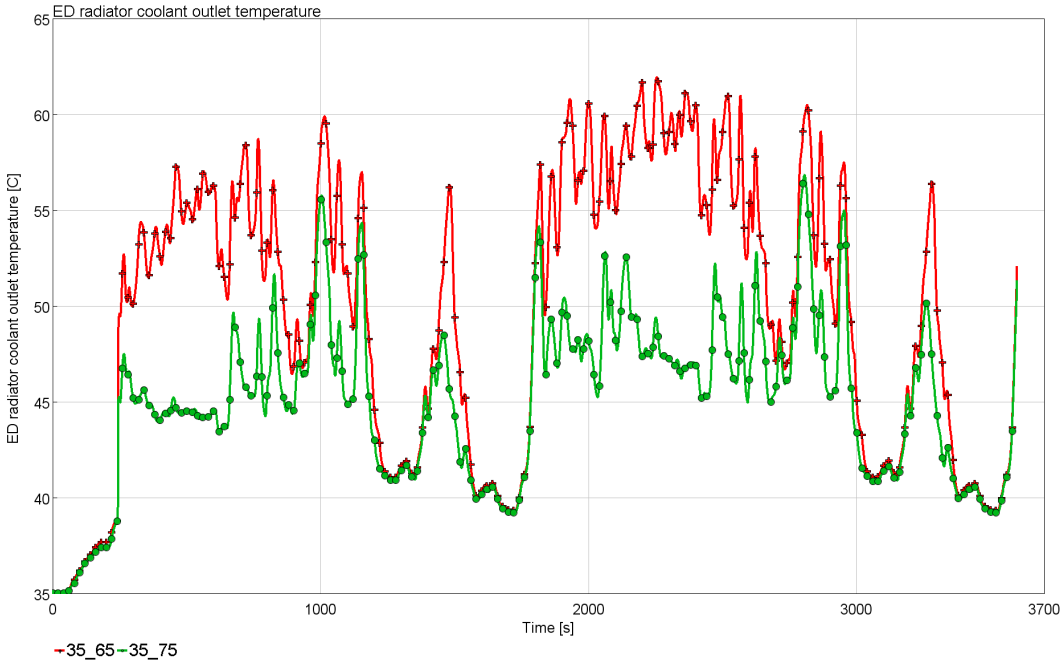

Figure 29: ED Coolant Radiator Outlet Temperature

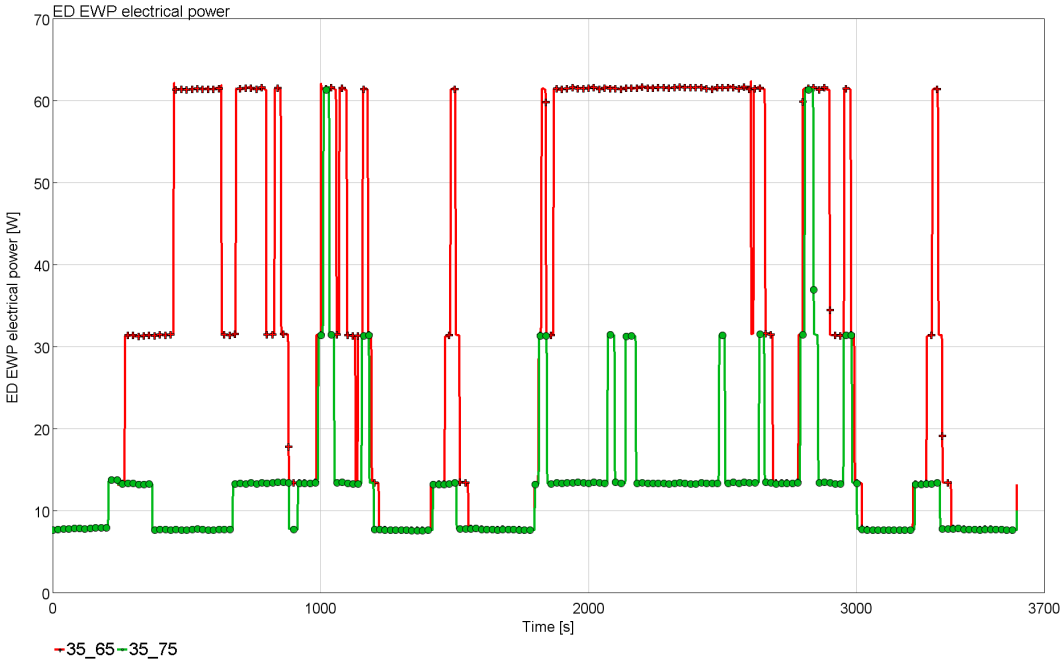

Figure 30: ED Electric Water Pump Power

From Fig. 30 the 35_65 case, the pump power fluctuates peaking to power values to about 60 W in the first half of both drive cycles for a longer period in the second drive cycle. The 35_75 case maintains consistently low power values of around 10 W with occasions of high peak values during the drive cycle. Relatively lower temperature are observed from the 35_75 case as compared to the 35_65. A similar trend is followed for the cases exhibiting large variations in the initial stage of each drive cycle with values stabilizing and showing lesser variations along each of the drive cycle. The absolute integral power is calculated from each component. The percentage difference from the base case is taken into account. The results are shown in Table 14. The cooling fan shows a great increase in power but the compressor and ED EWP display less power for the 35_75 case. There is an overall 17% decrease in power consumption for the 35_75 case from the base 35_65 case.

Case	Compressor (kWh)	Cooling Fan (kWh)	ED EWP (kWh)	Total (kWh)	Percentage Difference
35_65	1.405	0.018	0.033	1.456	-
35_75	1.125	0.059	0.012	1.195	-17%

Table 14: Integral Component wise and total power fan study results(kWh)

4.1.3 Ambient Temperature and Battery Cooling Change Study

Four cases are taken into account varying the ambient temperature and initial battery temperature. The compressor is the first component taken into account, with the compressor outlet pressure parameter taken. The compressor outlet pressure vs time plot is shown in Fig. 31.

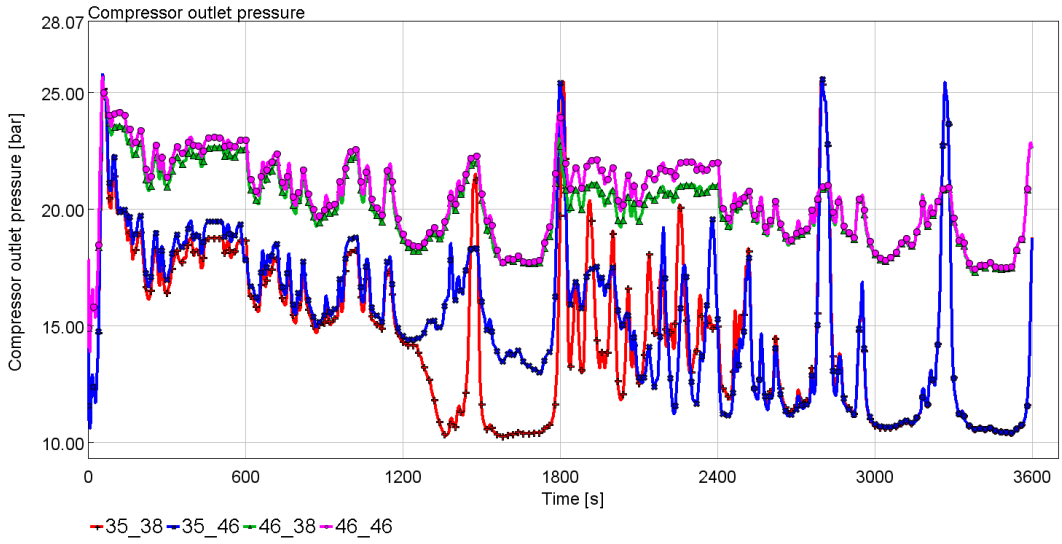

Figure 31: Compressor Outlet Pressure

From Fig. 31, the outlet pressure peaks to the maximum pressure of about 25 bar for the first 100 seconds and then drops along the first drive cycle. At the start of the second drive cycle the pressure increases and drops again. The 35_38 and 35_46 cases maintain similar pressure ranges consistently under 20 bar but the 46_38 and 46_46 cases maintain pressures above 20 bar. The highest pressure values are displayed by the 46_46 case and lowest pressure by 35_38 case. The next component is the cooling fan, the cooling fan power vs time is shown in Fig. 32.

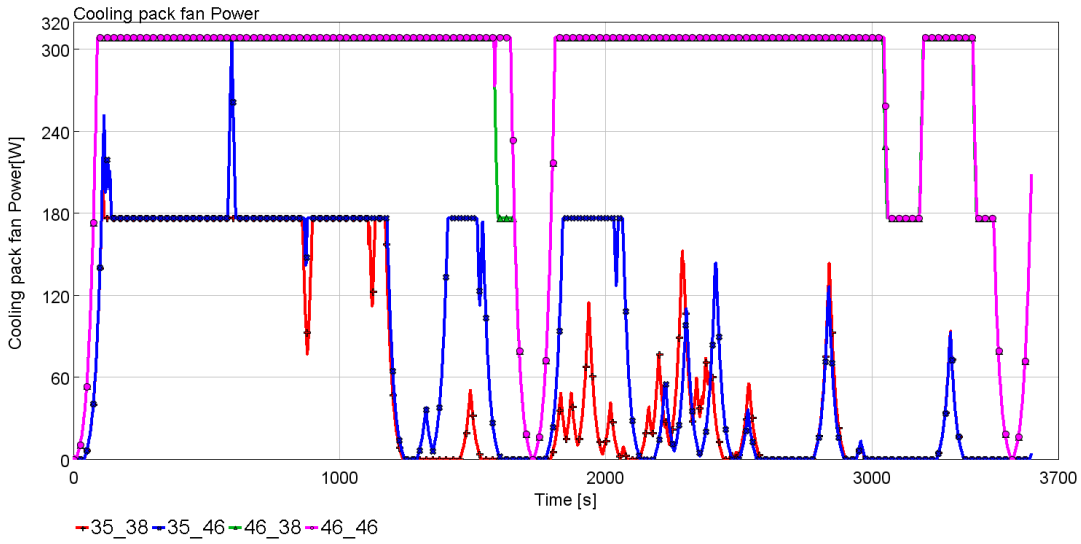

Figure 32: Cooling Fan Power

The cooling fan power maxes out at 180 W for the 35_38 and 35_46 case. The 35_46 peaks for higher power values for a longer period of time than the 35_38 case, followed by similar trends for both cases at the end of the drive cycle. The 46_38 and 46_46 show consistently high maximum power values of about 300W throughout the drive cycle bottoming in between the two drive cycles and then maxing out at the same value. The power drops then towards the end of the time period. The next component is the electric drive radiator, with the coolant outlet temperature plotted against time in Fig. 33.

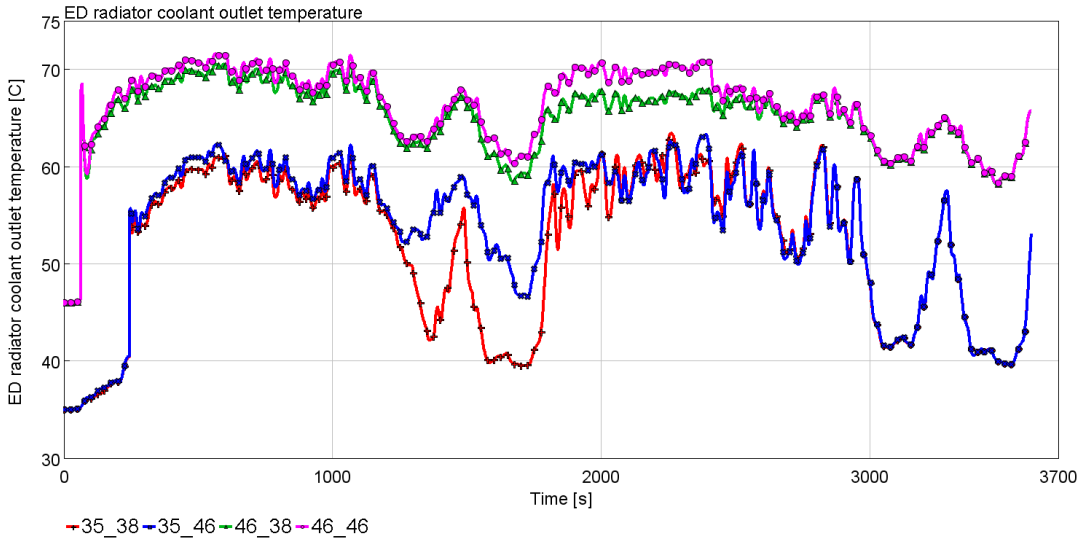

Figure 33: ED Radiator coolant outlet temperature

In both the drive cycles, the trends show increase in the temperatures followed by dropping to lower temperature values towards the end of each drive cycle. The 35_38, 35_46 peaks to temperatures less than 60°C and the 46_38, 46_46 over 60°C. The highest temperatures are shown by the 46_46 case and the lowest by 35_38 case which shows lower temperatures between the two drive cycles around the 1800-second mark. The ED EWP power plot is plotted next against time in Fig.34.

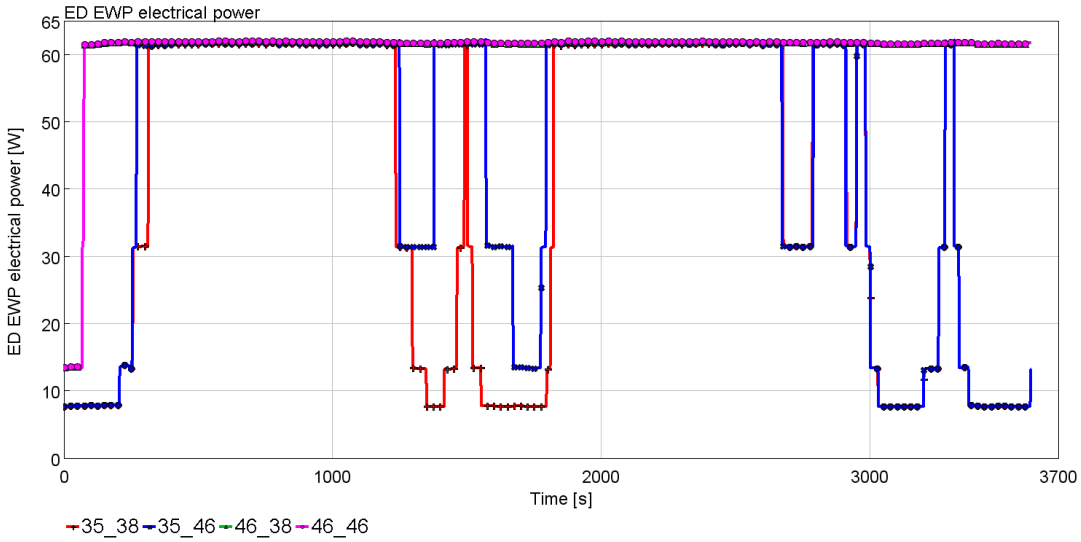

Figure 34: ED EWP Power

The pump is consistently at maximum power of 60 W for the entire time period for the 46_38 and 46_46 case. The 35_38 and 35_46 case shows high power at the first half of both drive cycles, then drops and peaks again towards the end of each drive cycle. The 35_46 case shows higher power than the 35_38 case. The battery EWP is the next component with the power plotted against time in Fig. 35.

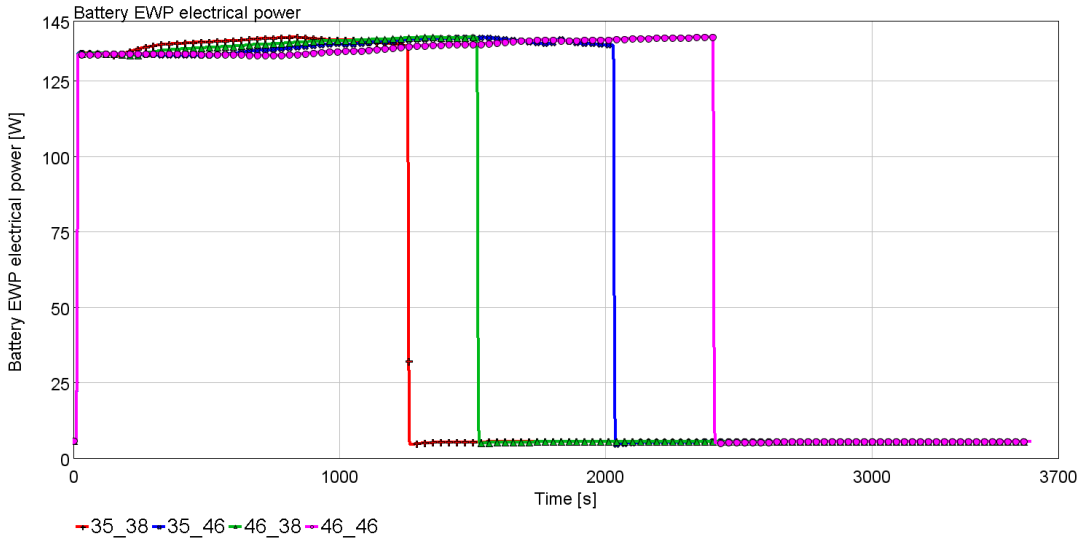

Figure 35: Battery EWP Power

The battery EWP power plot indicates it is at maximum power of about 135 W at the beginning of the drive cycle and then drops to 0W, eventually turning off showing no power in the remaining duration of the drive cycle. The 35_38 case power drops the quickest around 1200 seconds mark, followed by the 46_38, the 35_46 and lastly the 46_46 drops around the 2300 second mark. The averaged battery temperature is plotted against time in Fig. 36.

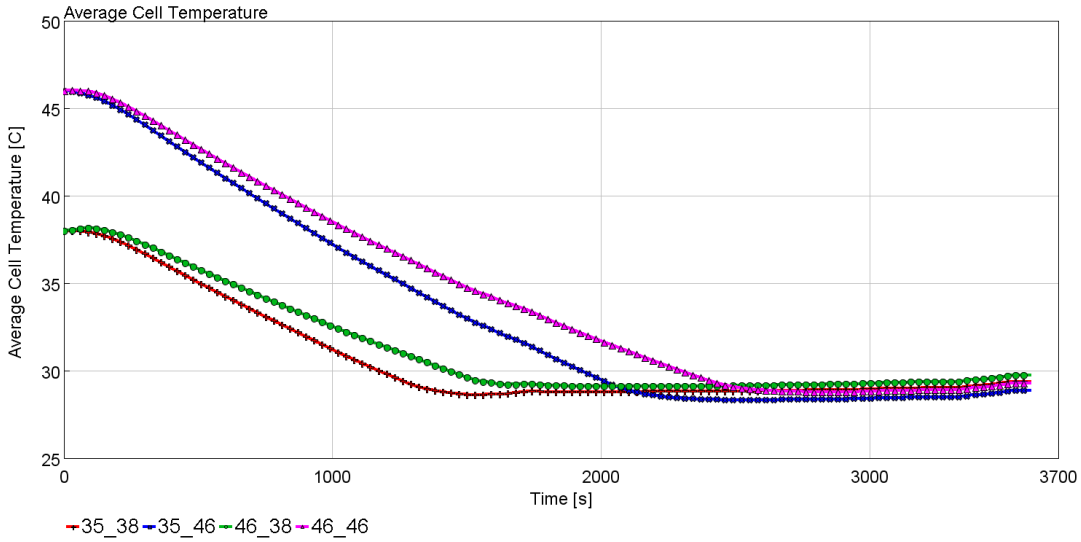

Figure 36: Battery Cell Temperature

The battery temperature starts at the initial 38°C for the 35_38, 35_46 cases and 46°C for the 46_38 ,46_46 cases. Over time it drops and stabilizes to the target temperature of 28°C. The two 35°C cases stabilize quicker to the target temperature compared to the 46°C cases that stabilize later.

The 46_46 case takes the longest time duration to reach the target temperature and the 35_38 case the fastest among all the cases.
The general trends of all the above plots show the highest values for the 46_46, followed by the 46_38 in similar ranges with next the 35_46 and finally the 35_38 values in similar ranges. The integral power values are calculated for each of the plots and the total power is summed up in kilowatt hours in Table15.

Case	Compressor (kWh)	Cooling Fan (kWh)	ED EWP (kWh)	Battery EWP (kWh)	Total (kWh)
35_38	2.120	0.051	0.038	0.049	2.258
35_46	2.669	0.066	0.041	0.077	2.853
46_38	3.985	0.258	0.060	0.059	4.362
46_46	4.225	0.261	0.060	0.090	4.636

Table 15: Integral Component-wise and Total Power Ambient Temperature and Battery cooling results(kWh)

On observing the overall power, the highest power is consumed by the 46_46 case and the least power in consumed by the 35_38 case. All the components follow the similar trend. The two 46°C cases show less difference in power compared to the 35°C cases. The cooling fan and ED EWP almost have similar range of power values, for the 46°C cases. There is less variation in power consumption with about 6% increase in power when the battery temperature of the 46°C is increased from 38°C to 46°C. For the 35°C cases there is a 26% power increase when the battery temperature is increased to 46°C.

4.2 Improvement of the thermal model with AGS Results

4.2.1 Cooling Fan Control Block Implementation Results

The results of the Cooling fan implemented with the additional fan control block is shown in Fig. 37.

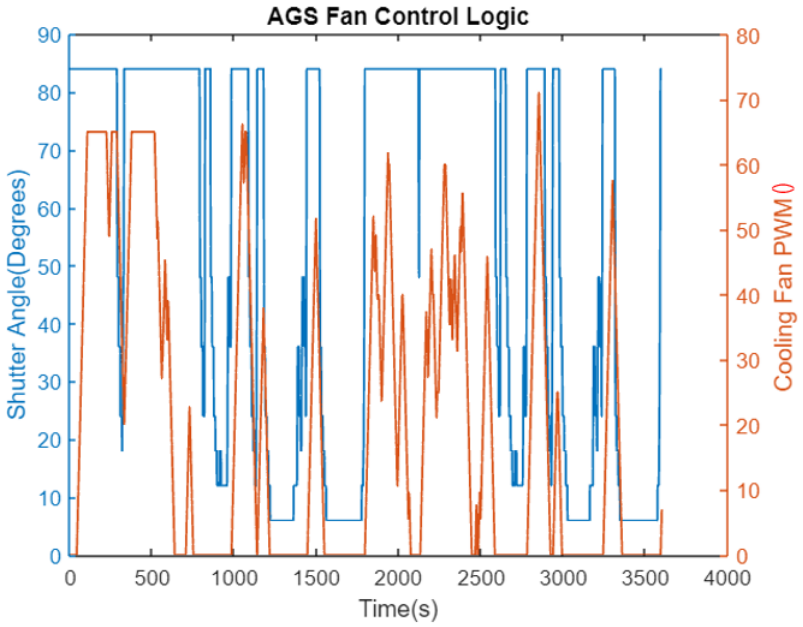

Figure 37: AGS fan control logic PWM

It is observed that the additional implemented block is successful in regulating the cooling fan speed, as in all instances when the grille shutters close, the fan tries to switch off. At points such as the 400-second mark where the cooling fan failed to close in Fig. 18 the updated logic seems to have fixed this with the cooling fan dropping to around the 25 PWM mark when the shutters close. Although at the same mark in the drive cycle, the fan does not switch off completely as the PWM does not drop to 0. This is as the shutter closes for a very short instance of time such that the fan needs to be turned on again when the shutters open. Therefore it is observed that the additional implemented block is successful in regulating the cooling fan speed, as in all instances when the grille shutters close the fan tries to switch off.

4.2.2 Manual Fan Control Implementation Results

Manual Fan control is implemented and the simulation is run with fan data derived from tests. The results for the mass flow rate through the condenser is observed along with the default case logic from GT-SUITE simulated earlier for comparison in Fig. 38.

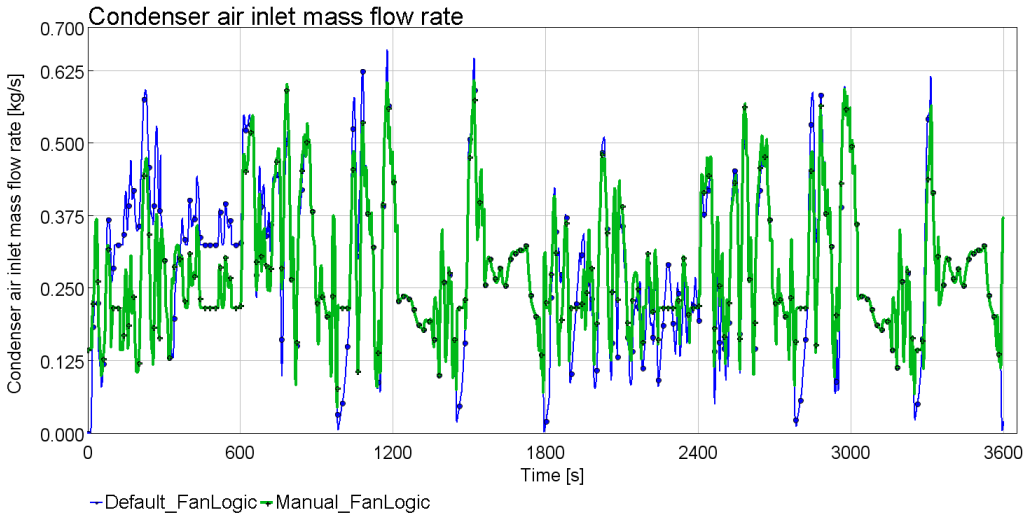

Figure 38: Mass flow rate condenser

The results indicate that at the various instances seen in the default fan logic from GT- SUITE where the mass flow rates drop to zero, for the manual fan control these values do not drop to zero. The manual fan logic which contains the correct fan PWM data implemented from tests. This ensures that the mass flow rate values do not drop to zero at any of the instances along the drive cycle. It is also observed that the mass flow rate for the manual fan logic shows a relatively lower mass flow rate before the 600-second mark. Post this mark the trends in the mass flow rate are relatively similar for both the initial default logic and the implemented fan logic. The mass flow rate peaks at lower values for the implemented manual logic as well.

4.3 Impact of Additional Mass Flow Rate on Energy Balance Study Results

The code outputs grille shutter angles and fan PWM values on input of the mass flow rates. These two values are then input into the thermal model in order to get the desired mass flow rates for the cases. First the grille shutter angles derived from the code are displayed in Fig. 39. The grille shutter angles vary based on the mass flow rate demand.

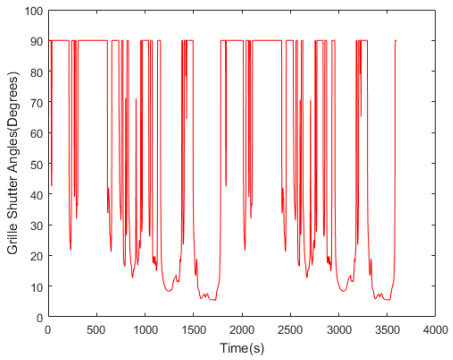

(a) Mass Flow Rate 0.3 kg/s

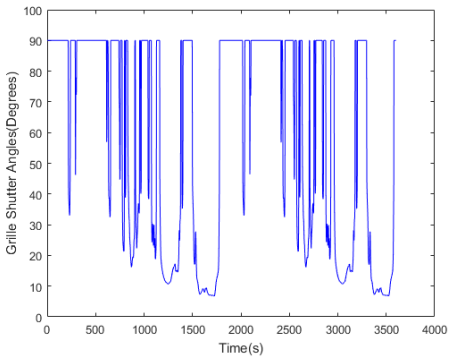

(b) Mass Flow Rate 0.35 kg/s

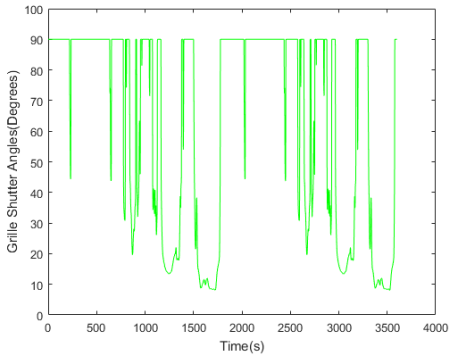

(c) Mass Flow Rate 0.4 kg/s

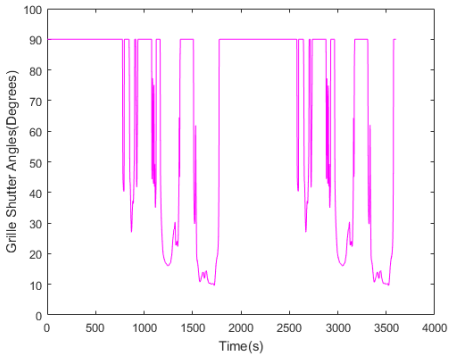

(d) Mass Flow Rate 0.45 kg/s

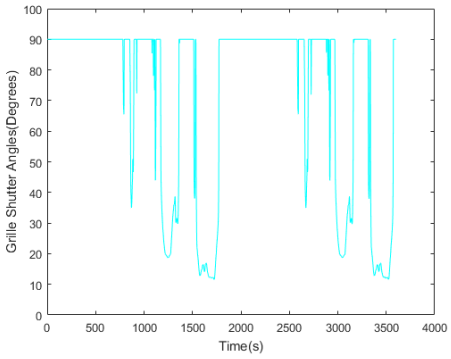

(e) Mass Flow Rate 0.5 kg/s

Figure 39: Shutter Angles

The grille shutters are fully open at 90° and fully close at 0°. The case with the minimum mass flow rate of 0.3 kg/s is observed to have the shutters closed at many instances along with the drive cycles, whereas for the case with the maximum flow rate i.e the 0.5 kg/s case the grille shutters are open the most instances. It is observed from the five plots to increase the mass flow rate in the system, the shutters open greater until they reach 90°. There are some common instances for the shutters closing in all cases. The 0.3 kg/s case also fully bottoms to the lowest grille shutter angles along the plot and with increasing mass flow rate, the cases bottom to greater shutter angles. Therefore to increase the mass flow rate along the cases, the grille shutter angles tend to open more until the fully open state. The next value derived from the code, the fan PWM plots are observed in Fig. 40.

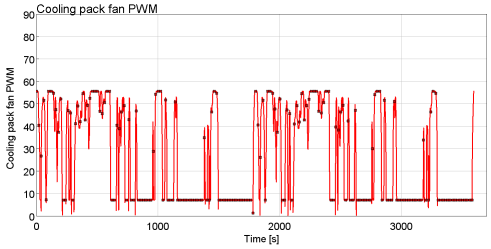

(a) Mass Flow Rate 0.3 kg/s

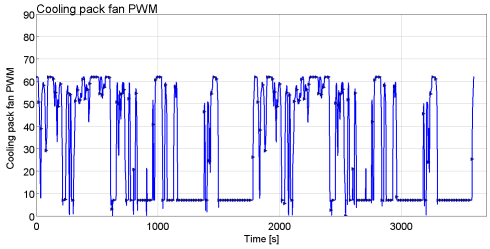

(b) Mass Flow Rate 0.35 kg/s

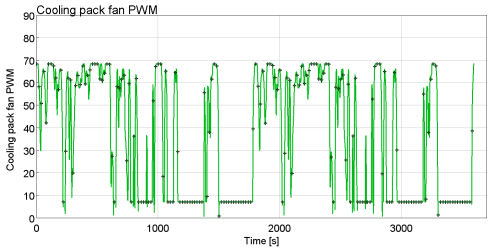

(c) Mass Flow Rate 0.4 kg/s

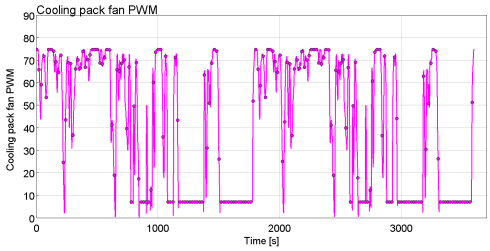

(d) Mass Flow Rate 0.45 kg/s

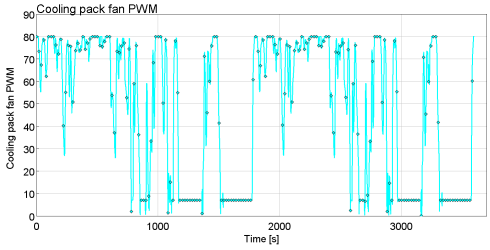

(e) Mass Flow Rate 0.5 kg/s

Figure 40: Fan PWM

All the mass flow rate cases show the same cooling fan PWM trends but different scales. The plots bottom at the same instances in all the plots. The five plots indicate to increase the mass flow rate the cooling fan needs to increase its speed. The trends show the lowest PWM for the 0.3 kg/s with the cooling fan maxing out at 55 PWM, there is a gradual increase in PWM across the cases with the mass flow rate. The 0.5 kg/s case displays the maximum PWM trends maxing out at 80 PWM which is the cooling fan limit.

The results are obtained after simulating the five cases with the above shutter angles and fan speed values. First, the mass flow rates are observed for all the five cases in the condenser in Fig. 41.

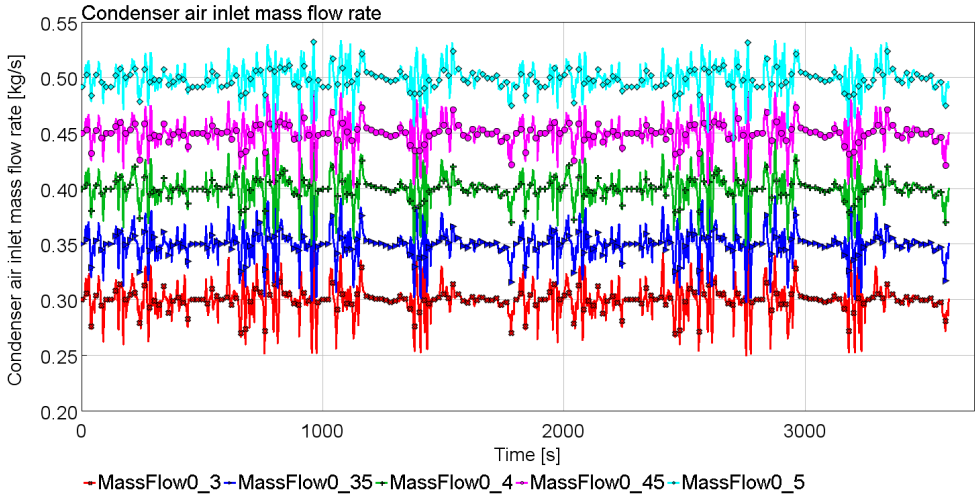

Figure 41: Additional Mass flow rates condenser

The mass flow rates derived including the fan and shutter variations, although input to run at a constant flow rate in the entire drive cycle observes fluctuations in the entire duration, do not remain constant throughout the simulation. The fluctuations are instantaneous over the entire time period. The variations are observed at the same instances for all the cases. The fan PWM and cooling fan values for observed for each case. The cabin temperature is observed for the various mass flow rates near the head of the left occupant. The temperature against time plot is shown in Fig. 42.

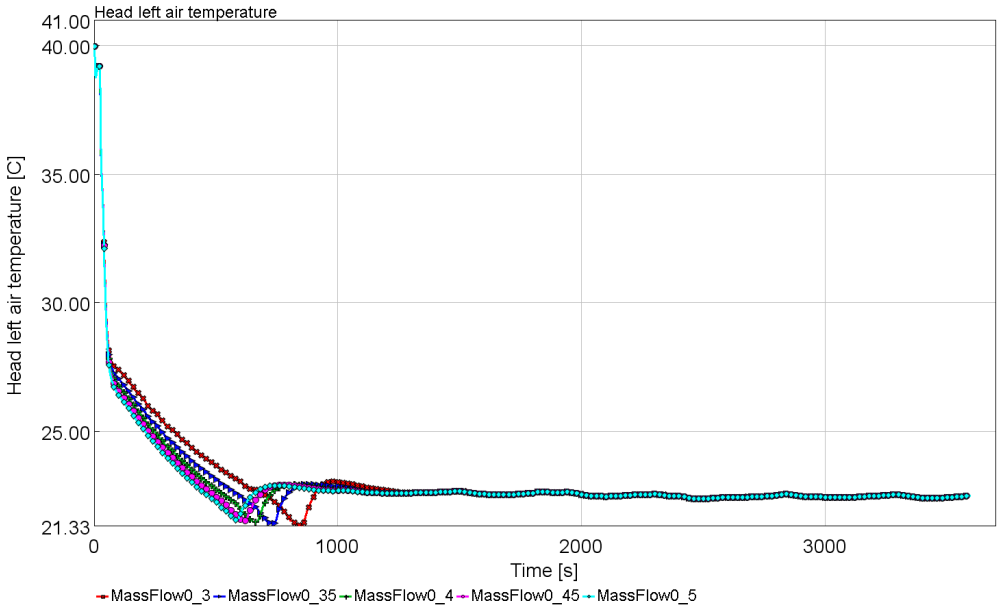

Figure 42: Cabin Temperature

The cabin temperature drops from an initial 40°C to 22°C. For all cases, the temperature drops to 21°C before the 1000 second mark increases and then stabilizes for the entire time period. With the increase in mass flow rate along the cases, it is observed that the temperature drop occurs faster. The fastest drop occurs for the 0.5 kg/s case and the slowest for the 0.3 kg/s case. Increasing the mass flow rate appears to accelerate the cooling of the cabin. Among the components of interest the compressor is observed with the compressor power against time plotted in Fig.43.

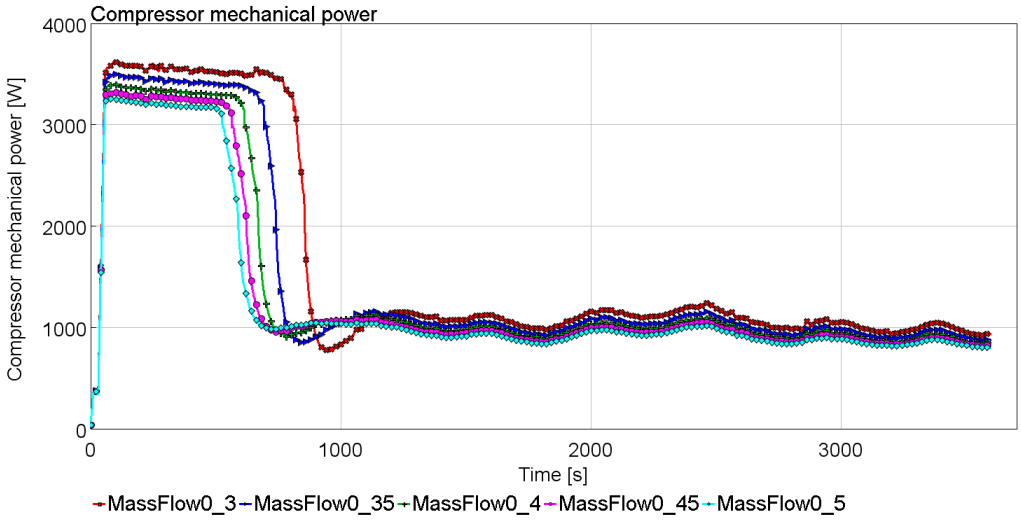

Figure 43: Compressor Power

Similar trends are observed across all cases where the compressor power increases and consistently runs at high power of about 3000 W until the power drops and stabilizes to around 1000 W post the 1500 second mark. The highest compressor power is observed in the 0.3 kg/s case and the power drops takes the longest time period among all cases to stabilize. It is observed that with the increase in mass flow rate for each case, the compressor power decreases. Hence among all cases, the 0.5 kg/s case displays the lowest compressor power along the drive cycles with the power stabilizing the quickest among all after the initial high power spike. Therefore the flow rate increase leads to less compressor use.
The Electric drive is observed with the electric drive coolant outlet temperature parameter taken into account as seen in Fig. 44. The trends indicate that the highest coolant outlet temperatures for each case are achieved in the initial first 1000 seconds of the drive cycle followed by stabilization of the temperatures to lower values in the rest of the time period. From the results it is observed that with increasing mass flow rate for each case, lower coolant radiator temperature trends are seen for the 0.5 kg/s case. The coolant at the ED radiator is discharged at lower temperatures with the increase in mass flow rate. The Electric Drive Electric Water Pump (ED EWP) is observed next with the power plotted against time in Fig. 45. The ED EWP plot for the 0.3 kg/s case shows that the pump is working at maximum power of 60 W for the entire time period, bottoming to lower power values at some instances in the drive cycles. The trend of the remaining cases show the pump at maximum power in the first 1000 seconds followed by a drop in power and varying low power values between the cases in the rest of the time period.

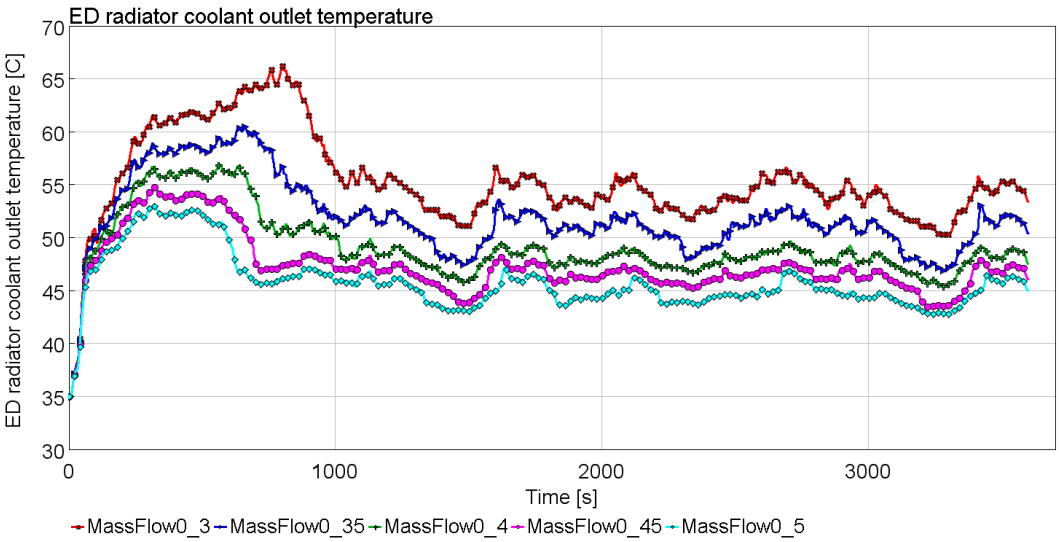

Figure 44: ED Radiator coolant outlet temperature

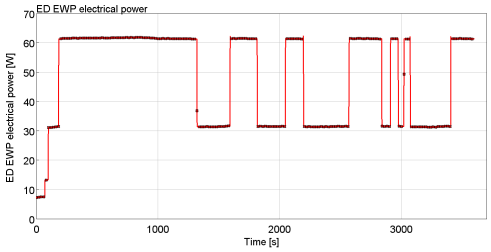

(a) Mass Flow Rate 0.3 kg/s

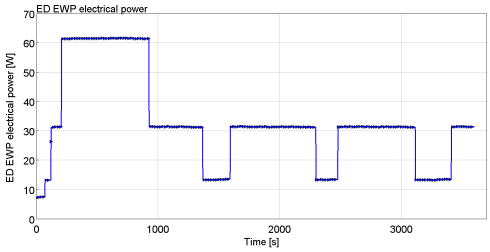

(b) Mass Flow Rate 0.35 kg/s

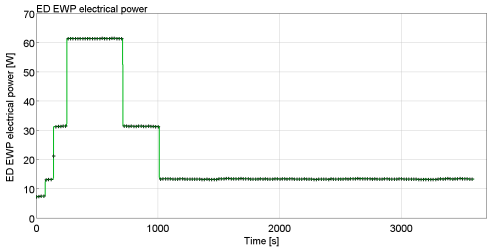

(c) Mass Flow Rate 0.4 kg/s

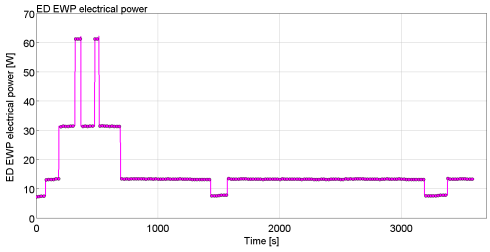

(d) Mass Flow Rate 0.45 kg/s

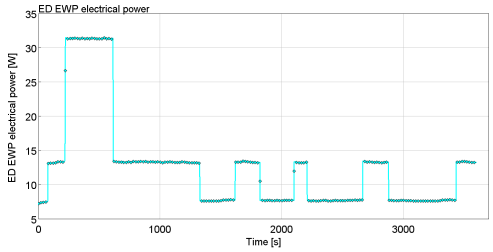

(e) Mass Flow Rate 0.5 kg/s

Figure 45: ED Electric Water Pump Power

As the mass flow rate is increased with every case, the pump is observed to use less power to regulate the flow of the coolant with the 0.5 kg/s case indicating the lowest power values of less than 10 W in many instances. This indicates that increasing the mass flow rate leads to reduction of ED EWP power consumption. The energy consumption due to the opening of the shutters is calculated and the plots are observed below in Fig. 46.

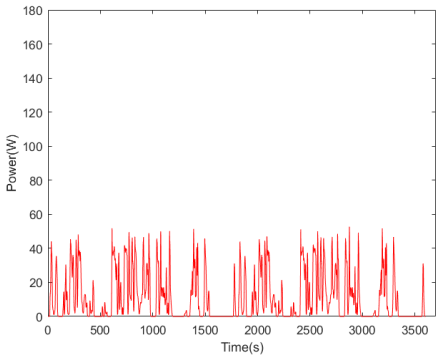

(a) Mass Flow Rate 0.3kg/s

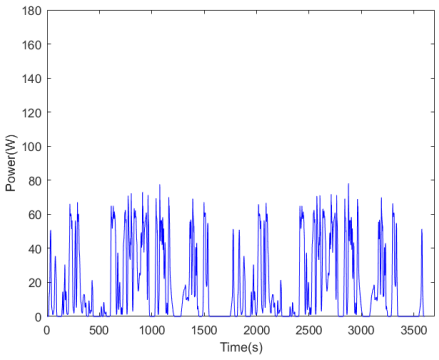

(b) Mass Flow Rate 0.35kg/s

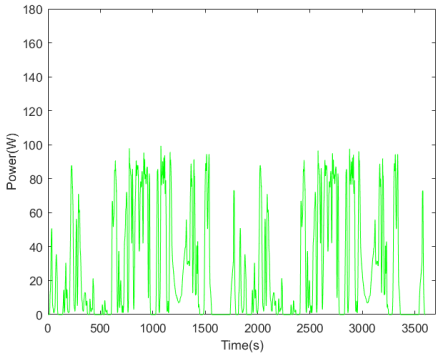

(c) Mass Flow Rate 0.4kg/s

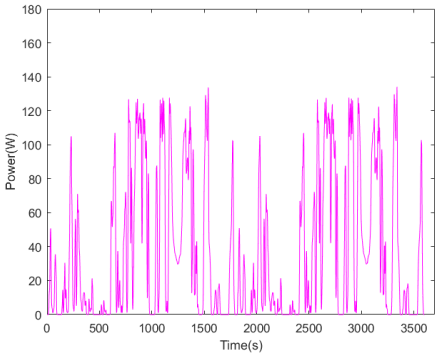

(d) Mass Flow Rate 0.45kg/s

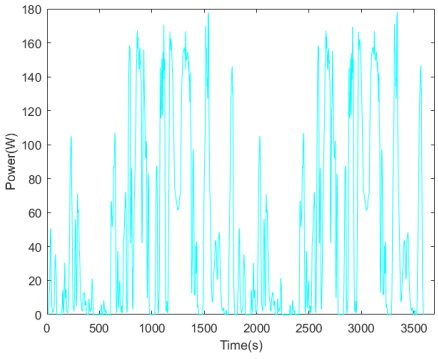

(e) Mass Flow Rate 0.5kg/s

Figure 46: Energy Consumption due to AGS

The power consumed is observed for the five mass flow rates. The trends along the drive cycles remain similar for all cases with instantaneous jumps in power that are observed constantly along the drive cycle with periods of bottoming at similar instances. The scales are different for each case, the power consumed seems to gradually increase with the increase in mass flow rate. The lowest power trends are observed with the 0.3 kg/s maxing out at around 40 W and the highest power observed for the 0.5 kg/s with values touching about 180 W. The integral power which is a single absolute value of the power along the entire time period of 3600 seconds of all the components of interest which are the compressor, cooling fan, and ED EWP is calculated. Additionally, the integral power due to the variation of the shutters are taken into account and added altogether with the components to calculate the total power consumption of the vehicle. The total power is shown in Table 16.

Case (kg/s)	Compressor (kWh)	Cooling Fan (kWh)	ED EWP(kWh)	Shutter Power (kWh)	Total (kWh)
0.3	1.592	0.051	0.048	0.012	1.694
0.35	1.457	0.059	0.033	0.024	1.573
0.4	1.368	0.082	0.021	0.039	1.510
0.45	1.306	0.111	0.015	0.055	1.487
0.5	1.260	0.146	0.012	0.074	1.492

Table 16: Integral Component-wise and Total Power Energy Balance Studies Results(kWh)

The integral values display that with increased mass flow rate, compressor and ED EWP power decreases . However, the power from the shutters variation and cooling fan seems to increase. The total power calculated indicates that with increasing mass flow rate the overall power seems to decrease up to reaching the 0.5 kg/s case, where the power starts to increase again. The next table displays the difference in power between each case in Table 17

Case (kg/s)	Total Power (kWh)	Diff.between each case (kWh)
0.3	1.694	-
0.35	1.573	0.121
0.4	1.510	0.063
0.45	1.487	0.023
0.5	1.492	-0.005

Table 17: Total Power Case by Case Difference(kWh)

It is seen that the difference in overall power seems to vary with each case. It is observed that between each case the power seems to decrease with increasing mass flow rate up to the 0.5 kg/s case, where the difference in power shows negative values indicating increase in power values.

5 Discussion

5.1 Sensitivity Analysis

The mass flow rate studies across the four cases showed plenty of variation in the power consumption of the vehicle. The high outlet pressure is an indication that the compressor is working harder. The trend of the compressor outlet pressure in Fig. 22 shows high-pressure values at the start of the first drive cycle as the cabin temperature of the vehicle is high and the compressor is working hard to bring down the cabin temperature to the desired target value. There is a greater discharge of the refrigerant to the condenser to absorb the higher amount of heated air. The velocity of the vehicle is also low at the start of each drive cycle and gradually builds up. Due to less ram air to cool the refrigerant as the vehicle is at low speeds, greater compressor pressure values are observed at the start. As the vehicle speed increases and the cabin is relatively cooled down, there is enough mass flow rate for the compressor to release the refrigerant gas at a lower pressure.

The compressor then bottoms once the temperature is brought down but then shows peaks of high pressure while maintaining the desired vehicle temperature in both the drive cycles. This is based on the drive cycle when the vehicle is at zero velocity, there is no ram air into the vehicle so the compressor needs to work more to provide sufficient cooling into the vehicle. The cooling fan gets its control logic from the compressor outlet pressure hence displays a similar trend as the compressor in Fig. 23. The cooling fan works at high power, in the beginning to bring down the vehicle cabin temperature by sucking in more air. In the cases where the flow rate is decreased (10 % decrease case), the vehicle cabin takes longer to cool down to the target temperature due to less ram air available. Hence, to compensate this the cooling fan runs for a longer duration. Once the vehicle cabin is sufficiently cooled the cooling fan is no longer needed to run constantly and just peaks when the vehicle is at zero velocity indicated by the peaks in the plots.

The electric drive radiator coolant outlet temperature shown in Fig. 24 depends on the mass flow rates through the radiator that cools the electric motor. Therefore when the vehicle is at high speed at the end of each drive cycle, the motor needs to power the vehicle more requiring greater cooling at the end of each drive cycle. The internal resistance is also higher in the motor at higher speeds which causes it to heat up, which places a larger demand on the amount of heat that needs to be rejected at the radiator. Therefore, due to this the radiator discharges the coolant at a higher temperature. The ED EWP works on the logic based on the electric radiator coolant outlet temperature hence showing the same trend of high power values with regions of bottoming when the vehicle is at high speeds in the drive cycle in Fig. 25. Based on the radiator coolant temperature the pump regulates the flow and when the temperature is high it uses more power to drive the coolant to exchange heat from the motor. The head left cabin temperature in Fig. 26 shows how the AC system tries to cool the cabin in the first drive cycle itself quickly within the first 1000 seconds and then maintains the temperature in the entire time period.

The mass flow rate changes impacts the power consumption as seen in Table13. The cases show the most variation after the initial peak when the temperatures of the vehicle stabilize. For all the plots the highest trends are shown for the case with the most decreased mass flow rate i.e the 10% decrease and this is indicated in absolute values. Due to the decreased mass flow, the compressor has to run faster to be able to reject the same amount of heat at the condenser. This is followed by the next decreased case which is the 5% decrease, then the increased case of 5% and 10% increase case which consists of the lowest trends of all. In this case as the vehicle lacks the ram air the components work hardest of all the cases. The cabin temperature plots indicate the cooling of the cabin takes place quicker for the higher mass flow rate case (10% increase case). The extra ram air facilitates better heat transfer from the cabin. The 10% increase shows slight instantaneous changes for the pump power values due to the coolant temperature of the radiator dropping below a temperature that runs the pump at less than the threshold value that is indicated in the logic.

On observing all the individual power consumption values, the compressor consumes the most power among all components as it initiates the heat transfer cycle squeezing the refrigerant to increase its temperature. Therefore it is a key component in reducing the power consumption of the vehicle. The compressor power consumption is known to be proportional to the indexed compression ratio, also known as the ratio of discharge pressure to suction pressure. The power consumption increases as the compression ratio increases as the discharge pressure rises. Overall the increase in mass flow rate is observed to provide savings in energy consumption with the extra mass flow rate causing to components to work less and the decrease in mass flow rate causing the components to work more. Therefore increasing/decreasing the mass flow also causes significant changes in the power consumption of thermal components of the vehicle.

The fan study shows that varying the cooling fan speed can greatly affect the power consumption of the vehicle. The plot trends follow the same as for the mass flow rate study in the case where the fan is at 65 PWM. However, when the fan speed is increased to 75 PWM low trend values for the compressor, EWP, and high cooling fan power are observed. This is due to the cooling fan working harder to bring in extra airflow to facilitate better heat transfer, causing the compressor and pump to work less. Hence, needing the components to discharge the refrigerant and coolant at less pressure. This cooling as shown in the plots is sufficient also when the car is at low speeds also shows the regions in the initial stages of each drive cycle. The values rise when the vehicle is at zero velocity. The power consumed by the cooling fan is less compared to the compressor, which consumes the most energy. This extra airflow causes higher inlet air flow into the heat exchangers, therefore sees a drop in overall power consumption upto 17%. However, an increase in cooling fan speed could lead to Noise Vibration Harshness (NVH) related issues which are out of the scope of this thesis to investigate.

The battery cooling and ambient temperature increase study consisted of two ambient temperatures and two battery temperatures across four cases. Increased ambient temperature lowers the density of the inlet air, thus reducing the mass flow. The two higher ambient temperatures cases of 46°C show a higher compressor discharge pressure in Fig. 31 due to the more workload of bringing down the high ambient temperature. This would need to discharge the refrigerant at a much higher pressure to cool down the vehicle. The same is said for the initial battery temperatures, with the higher initial battery temperatures requiring higher pressure to be discharged for the refrigerant to be circulated for battery cooling. The cases with the same ambient temperatures and different battery temperatures seem to give similar trend values along the time period based on the cases as the battery temperatures are sufficiently cooled to the desired temperatures by then. This is indicated in the cell temperature plot in Fig. 36 as well that the battery gets sufficiently cooled to its target temperature in the drive cycle. The battery cooling time is based on how high the initial battery temperature is and the ambient temperature. The cooling fan as seen in Fig. 32 for the 46°C ambient temperatures cases are consistently at high power due to the temperature of the cabin being very high requiring the air to flow in constantly through the heat exchangers. At the end of each drive cycle, the vehicle cabin is cooled sufficiently to its target temperatures when the fan power drops.

For the cases with the higher initial battery temperatures to cool the cabin, the fan stays on at higher power consistently at 300 W even in the second drive cycle. For the electric drive, the radiator coolant outlet temperatures are higher for 46°C cases. This causes the ED EWP to work at maximum power throughout the drive cycle to regulate the coolant flow to the motor for these cases and to maintain the desired target temperatures as seen in Fig. 34. The battery EWP indicated in Fig. 35 shows that the pump needs to be at maximum power for the longest time duration to regulate the coolant flow. Hence delivering the coolant at a high flow rate to facilitate heat exchange of the battery for the highest battery temperature and highest ambient temperature case i.e the 46_46 case. The absolute values of the individual component power consumption show more variation and discrepancy up to almost 0.6 kWh between the 35°C cases especially for the cooling fan and pump values. This is due to these components working at their maximum designated limits in the model for the two 46°C cases.The different initial battery temperatures providing little changes, which also translates to little power consumption difference between cases. The overall power consumption indicates with the higher ambient temperature and higher battery temperature the cooling load increases which causes more energy consumption from the components.

The results of the sensitivity studies gave a good idea of the various operating points of the components of interest for the next studies. The overall goal is for energy savings in the system. For the future method improvements in the thesis, the results from this study is taken into account. Increasing mass flow rate leads to energy savings so this is further investigated with AGS implemented. The cooling fan increase in speed leads to total power savings as well, so the fan control optimization is observed in the system further.

For the rest of the study, the ambient temperature of 35°C is taken to not to run the components at their limits. This temperature also served as a good ambient temperature to cool down the cabin for the cool-down case studies. Battery cooling is no more taken into account for future studies as the previous study showed only being an added load case, which on cooling the battery just behaves similarly to the case without battery cooling. It is also observed that the battery EWP is not a very large consumer of energy in the system. Additionally, this is also done for simplicity to take fewer components into account for the next optimizations.

5.2 Improvement of the model with AGS

The Active Grille Shutters (AGS) needed to be implemented in the model for the complete vehicle thermal model to vary the grille shutters just like it would in the actual vehicle. Along with this the cooling fan control logic needed to be changed to accommodate the AGS.

The model need to be improved to produce more accurate cooling fan PWM results. The cooling fan if not operated based on the opening and closing of shutters could cause errors in the estimation of the power consumption of the thermal management system. The shutters close when there is no cooling required by the ram air for the thermal management system, hence running the cooling fan would also lead to additional wastage of energy. On implementation of the if-else control block, the fan PWM results seen in Fig. 37 successfully regulates the signal. Now when the shutter angles are not fully open, the fan starts to switch off establishing a connection with the variation of the shutter angles and fan PWM.

Manual fan control is implemented due to the fan not starting quick enough resulting in the mass flow rate dropping to zero, when the vehicle stops in the drive cycle. Although the controller in the thermal model senses a need to switch on the fan when the vehicle velocity is low and the grille shutters open, there is a delay for the fan to start again. This causes the mass flow rate to drop to zero. The fan PWM from tests used in manual fan control does not peak to high values or drop completely to zero compared to the PWM from the default fan control from GT-Suite. This results in a smaller gradient allowing the controller enough time to switch on the fan when the velocity of the vehicle slows down ensuring continuous airflow through the thermal management system as seen in Fig. 38.

A further better method needed to be devised as data from tests needed to relied on for fan speed values and also the grille shutters are fixed to the input. The mass flow through the heat exchangers also needed to be based on varying grille shutters angles and fan speed. Hence a code is developed based on mass flow rate input, grille shutter angles, and fan PWM data can be generated to input into the model. Now based on the input of these values in the model the vehicle behaves as close to the real vehicle where the air flow is also regulated by AGS and fan speed.

5.3 Impact of Additional Mass Flow Rate on Energy Balance Study

The code outputs shutter angles and fan PWM based on the mass flow rate input as shown in Fig. 39 and Fig. 40. The shutter angles tend to open further with an increase in mass flow rate to allow the increase in airflow into the thermal management system. When the shutters are moved from completely open to fully closed, the airflow volume through the heat exchangers and into the system decreases. In the fully closed position the air flow is reduced to almost zero, except for some minimal amount of airflow caused by leakages. The opening of the shutter at a larger number of instances allows the desired increase in mass flow. The instance along the drive cycles where the shutters are closed for all cases is when the vehicle is at high speed, making it essential for the shutters to close. This reduces the impacts of aerodynamics drag. Therefore the highest mass flow rate case sees the greatest number of instances in shutters opening. The fan PWM is also observed to increase in PWM scale with increasing mass flow rate. This is due to the fact to bring in more volume of air the cooling fan would need to increase its speed. As the fan rotates, the rotating air flows away from the hub, generating a partial vacuum that allows additional air to flow into the fan. The instances where the cooling fan speed bottom for all cases is when the grille shutter is closing. Once the grille shutters are open to their limits, the cooling fan brings in more airflow to achieve the desired mass flow rate. The lowest mass flow case of 0.3 kg/s is observed to have the lowest fan PWM values as the lowest mass flow rate is need to be achieved hence the fan runs at the lowest speed among all cases.

Although the values are input to run at the constant single mass flow rate for the entire simulation, the results from the model show transient behavior for the mass flow rates in Fig. 41. This is because the shutter angles and cooling fan regulate the mass flow through the heat exchangers. Therefore, causing the flow rate to frequently fluctuate based on the variations due to the vehicle velocity. This also complements controller delays for some time at points to regulate the mass flow rate at the desired value. The cabin temperature observed in Fig. 42 indicates a faster temperature drop with an increase in mass flow rate. The cabin is brought down to the temperature in the first 1000 seconds and then regulated by the thermal management system to keep it at the desired target temperature of 22°C. Due to the vehicle following the same drive cycle for all cases, the extra mass flow rate in the system causes an acceleration in cabin cooling as the cool air initiates better heat transfer and dissipation of heat. Further investigations would need to be made to understand the potential energy gains by following a similar cabin cool-down profile in all cases.

The Compressor in Fig. 43 shows high power up to 3600 W in the initial stages of the drive cycle due to a high cooling load of bringing down the cabin temperature from 40°C. In the first 1000 seconds for all cases, the compressor is at high power to bring down the cabin temperature to its desired target temperature. After it achieves the target cabin temperature, the compressor power stabilizes and works to keep the desired temperature for the remaining time period.

The compressor power trends seem to decrease with increasing mass flow rate. The increasing mass flow enables a higher amount of heat to be rejected at the heat exchangers. Therefore the compressor needs to work less to reject the same amount of heat. Hence the compressor work at lower power to discharge the refrigerant to the condenser.

The higher cooling load in the first drive cycle is again highlighted where the coolant temperature is higher for the first WLTC cycle and stabilizes in the second drive cycle. The increase in flow rate allows the coolant to be discharged from the radiator at lower temperatures with the increase in airflow helping in bringing down the coolant temperature. The electric drive electric water pump (ED EWP) indicates that the increase in mass flow rate helps in reducing the pump work in circulating the coolant. The logic for the ED EWP pump is derived from the ED radiator coolant outlet temperature. The 0.3 kg/s case plot indicated in Fig. 45 shows that the pump is continuously working at high speed due to the coolant outlet temperature crossing 54°C constantly in the whole time period. This is indicated by the ED EWP control logic shown in CVTM Theory.

The power consumption in Fig. 46 due to the opening of the shutters indicates that with increasing mass flow rate, the power consumption is higher. This is due to the shutters opening further while increasing the mass flow rate. When the AGS is fully closed, the air flows around the car rather than into the underhood bay, resulting in less aerodynamic drag than when the AGS is open. To overcome the aerodynamic resistance caused by opening the shutters, more power is used. Hence the highest power is consumed by the 0.5 kg/s case where the grille shutters are open the most.

The overall power consumption indicates with the increase in mass flow rate the power consumption decreases up to the 0.5 kg/s where it starts to increase again. The decrease takes place due to the major sources of power consumption that is the Compressor and ED EWP decreasing. The power from the shutter and cooling fan increase with increasing mass flow rate but they are not as significant contributors to the energy consumption as the compressor and ED EWP. However, on reaching the 0.5 kg/s case the power due to shutters opening overcomes the savings seen by the other components causing the overall power consumption to start increasing. The components of interest do not vary as much with the increase in flow rate due to the cooling fan reaching its component working limits. It is indicated by the power difference between each case when the difference in power between each increasing mass flow rate decreases until the last 0.5 kg/s case. Beyond this case, increasing the mass flow rate is no longer effective in decreasing the overall power consumption of the components in the vehicle.

6 Conclusion

The method described in the thesis involved improved prediction of results in the 1-D thermal model for the thermal management system components. This will help engineers come up with improved strategies for balancing the operating points of components, that will ultimately aid in designing more energy-efficient systems. The initial sensitivity studies indicate that with increasing mass flow rate, the power consumption decreases due to the compressor which is the most power-consuming, component consuming less power. It was also observed that increasing the cooling fan speed leads to additional power savings, as the cooling fan can compensate for the compressor work at a significantly lower overall power conversation. The higher ambient temperatures with battery cooling cases cause a significant load on the thermal management system. They observe smaller deviations in the power consumption between the cases, due to the components working at their limits throughout the drive cycles.

The active grille shutters are implemented in the thermal model for aerodynamic benefits at high speed. The model is improved to predict more accurate behavior. With the help of the implemented method by using the code, the vehicle mass flow rate in the thermal management system is regulated by the varying grille shutters and fan speed as well. These optimizations result in the model performing as close to like the vehicle would in real life leading to better energy predictions. This showed that by applying 1D-CFD modeling methodologies, the thermal management system may be efficiently optimized.

The impact of additional airflow on the power consumption to the optimized model with AGS, which included the power consumption of opening shutters is seen that with increasing mass flow rate there is a decrease in power consumption due to compressor, pump significantly working less. However, this decrease is until a point with the 0.5 kg/s case where the savings seen from compressor and pump are overcome by the increase in energy consumption by the opening of the grille shutters, where it is no longer seen effective to increase the mass flow rate through the thermal management system.

7 Future Work

This research can be improved by optimizing the model further for better energy predictions as well. The control strategies of other components in the model can be investigated by taking more components from the thermal management system. With the help of discoveries from this study, better control strategies can be developed between the grille shutters and thermal management system based on the amount of airflow into the vehicle. This would lead to additional energy savings in the model from the thermal management system. It was observed that the cabin cooling is accelerated with mass flow rate, the model can be cross-examined if there is a necessity for this to take place as the energy involved for this to take place can be conserved. The effects of aerodynamics can also be further explored more on how it affects the thermal management system cooling performance at different vehicle speeds and driving scenarios. The extra airflow brought in for cooling purposes can be evaluated so that the AGS can be controlled in a way so that both the aerodynamic drag and power consumption due to the compressor can be minimized for maximum power savings.
Studies can also be performed on a large number of cases such as heating up cases, where the vehicle is at low temperature and needs to be brought up to a high temperature. Various initial conditions such as charging scenarios like fast charging, etc could bring about further changes in power consumption. Several other driving scenarios can be taken into account with different drive cycles for variation in driving conditions.

References

[1] Gates B. How to Avoid a Climate Disaster: The Solutions We Have and The Breakthroughs We Need. Penguin Random House, LLC. Copyright; 2021.

[2] Commission E. A European Strategy for low-emission mobility; 2021. https://ec.europa.eu/clima/eu-action/transport-emissions_en.

[3] Josh Miller CB. Transport Could burn up the entire EU budget; 2021. https://theicct.org/blog/staff/eu-carbon-budget-apr2021.

[4] IEA. Global EV Outlook; 2016. https://www.iea.org/publications/freepublications/publication/Global_EV_Outlook_2016.pdf.

[5] Lin W SB. Vehicle Cooling Systems for Reducing Fuel Consumption and Carbon Dioxide. SAE Technical Paper Series; 2010.

[6] EnginsoftUSA. CFD; 2021. https://enginsoftusa.com/1-d-system-level.html.

[7] A El-Sharkawy JK, Rahman S. Evaluation of Impact of Active Grille Shutter on Vehicle Thermal Management. SAE International; 2011.

[8] Helena Martini LL P Gullberg. Aerodynamic Analysis of Cooling Airflow for Different Front-End Designs of a Heavy-Duty Cab-Over-Engine Truck. SAE International; 2018.

[9] Arevalo A, Han C. Air Conditioning System Modeling for Car Fuel Economy Simulation. KTH Royal Institute of Technology; 2018.

[10] K Okamoto MO H Aikawa, Hayashi K. Thermal Management of a Hybrid Vehicle Using a Heat Pump. SAE Technical Paper; 2019.

[11] Dinakar P, Rajeeve G. Modelling and Simulation of Cooling Systems for BEV High Voltage Battery. Chalmers University of Technology; 2016.

[12] Natarajan S, Mirzabeygi P. Impact of Active-Grille Shutter Position on Vehicle Air-Conditioning System Performance and Energy Consumption in Real World Conditions. SAE International; 2020.

[13] Bouilly J. Evaluation of Fuel Economy Potential of an Active Grille Shutter by the Means of Model Based Development Including Vehicle Heat Management. SAE International; 2015.

[14] Nordin J. CFD Study of Optimal Under-hood Flow for Thermal Management of Electric Vehicles. Chalmers University of Technology; 2017.

[15] Yang K. Impact of Front-end Air Flow Conditions end Air Flow Conditions on AC Performance and Real-World Fuel Economy. University of Windsor; 2018.

[16] HK Versteeg WM. An Introduction to Computational Fluid Dynamics. Longman Scientific and Technical; 1995.

[17] Bakker A. The Colorful Fluid Mixing Gallery. http://www.bakker.org/cfm; 2021.

[18] Gamma T. GT-SUITE Flow Theory Manual. Gamma Technologies LLC; 2020.

[19] WIEN T. Classification of Simulation Processes; 2008. https://www.iue.tuwien.ac.at/phd/spevak/node9.html.

[20] IV JHL. A Heat Transfer Textbook. Phlogiston Press; 2020.

[21] Branson J. Quantum Physics 130; 2013. https://quantummechanics.ucsd.edu/ph130a/130_notes/node48.html.

[22] James U. Thermal Radiation; 2010. https://phas.ubc.ca/~james/teaching/phys333/module1_lesson3.pdf.

[23] University KS. Basic Aerodynamics. Kazimieras Simonavicius University; 2017.

[24] E L Houghton SHCDTV P W Carpenter. Aerodynamics for Engineering Students (Seventh Edition). Elsevier; 2017.

[25] Gmbh RB. Bosch Mobility Solutions; 2014. https://www.bosch-mobility-solutions.com/en/solutions/thermal-management/thermal-management-for-hybrid-systems-and-electric-drives/.

[26] Lucile B PW. Investigation of new concepts of Active Shutters for Battery Electrical Vehicles. Chalmers University of Technology; 2019.

[27] Gamma T. GT-SUITE; 2020. https://www.gtisoft.com/.

[28] Linderoth J. Thermal Management of a Battery Electric Vehicle. Chalmers University of Technology; 2021.

[29] Inc E. Worldwide Harmonized Light Vehicles Test Cycle (WLTC); 2021. https://dieselnet.com/standards/cycles/wltp.php#:~:text=The%20Worldwide%20harmonized%20Light%20vehicles,Energy)%20group%20%5B26245D%20.

[30] Markowitz M. Minimising total vehicle energy consumption by balancing the aerodynamic of an active grille shutter and the power consumption of the air conditioning compressor. SAE International; 2011.